The HIRLAM model

Nils Gustafsson

Swedish Meteorological and Hydrological Institute
S-60176 Norrköping, Sweden

1. Introduction

THE HIRLAM Level 1 System is a complete system for short-range numerical weather prediction including a HIgh Resolution Limited Area Model based on grid-point representation, an objective analysis scheme based on statistical interpolation, a non-linear normal mode initialization scheme, pre- and postprocessing packages. The parameterization package of the model includes stratiform and convective condensation, turbulent transports, short-wave and long-wave radiation and surface exchange processes. The system was developed within a common research effort among the weather services in the Nordic countries and the Netherlands. The HIRLAM Level 1 system has been used operationally since January 1990 by the Finnish Meteorological Institute and since October 1990 by the Danish Meteorological Institute. Verification of operational forecast products indicate a forecast quality comparable to that of similar products from major European numerical forecasting centers.

Further development of the HIRLAM system is coordinated through the HIRLAM 2 project. In addition to the weather services mentioned above, the Irish Meteorological Service is a member of the HIRLAM 2 project. The main efforts during HIRLAM 2 have been spent on improving the performance and efficiency of the HIRLAM forecasting system. Major areas of research and development work are Semi-Lagrangian advection schemes and a new condensation scheme based explicit forecasting of the cloud water content. Another intention with HIRLAM 2 is to move towards mesoscale forecasting. Early applications of the HIRLAM Level 1 system at mesoscale resolutions have indicated promising skill.

In the presentation the main features of the HIRLAM Level 1 system will be described in some detail, the performance during the first year of operational application will be reviewed, some examples of very high resolution forecasts will be shown and a new version of the HIRLAM model, based on a spectral representation, will be described.

2. The HIRLAM Level 1 System

The HIRLAM Level 1 data assimilation and forecasting system consists of the following components:

(1) The numerical forecast model
(2) The non-linear normal mode initialization scheme
(3) The statistical interpolation objective analysis scheme
(4) Pre-processing of lateral boundary condition fields
(5) Post-processing of analysis and forecast fields to pressure levels
(6) Forecast verification against analyses and observations
(7) Preparation of orography and surface climate fields

Three main components of the HIRLAM Level 1 system are the forecast model, the initialization scheme and the objective analysis. These three components are described briefly in subsections 2.1 - 2.3 below. The pre- and post-processing packages are additional important components of the HIRLAM Level 1

system. Here should only be mentioned that some efforts were spent on developing techniques for preparation of lateral boundary conditions being as accurate as possible by direct vertical interpolation from the model levels of the large scale forecast model providing the boundary conditions to the model levels of the HIRLAM model. This interpolation is carried out with the emphasis to preserve e.g. boundary layer structures of the large scale forecast (Majewski 1985). A detailed description of the HIRLAM Level 1 system is given in the HIRLAM Documentation Manual (Källberg 1989).

2.1 The forecast model.

The HIRLAM Level 1 model is a primitive equation model using a grid point representation with second order difference approximations for the spatial derivatives. The prognostic variables are the horizontal wind components, the temperature, the specific humidity and the surface pressure. In addition, surface temperature, surface wetness and snow depth are predicted over land. For the time-stepping, a semi-implicit scheme is utilized.

2.1.1 Basic model equations and numerical formulation.

Basic model equations

The forecast model equations are written down for Hxgeneral pressure based and terrain following vertical coordinate $\eta(p, p_s)$ where

$$\eta(0, p_s) = 0 \qquad \text{and} \qquad \eta(p_s, p_s) = 1 \tag{2.1.1.1}$$

The formulation corresponds to the hybrid system used at ECMWF (Simmons and Burridge, 1981), with some modifications because the continuity equation is integrated upwards in the HIRLAM model.

The model is programmed for a spherical coordinate system (λ, θ), but in the formulation and in the code two metric coefficients (h_x, h_y) have been introduced. This is done to prepare the model for any orthogonal coordinate system or map projection with axes (x,y). For a distance $(\delta X, \delta Y)$ on the earth, it yields that

$$\delta X = a h_x \delta x \qquad \text{and} \qquad \delta Y = a h_y \delta y \tag{2.1.1.2}$$

In case of spherical rotated coordinates, we have that

$$\delta X = a \cos\theta \delta\lambda \qquad \text{and} \qquad \delta Y = a \delta\theta \tag{2.1.1.3}$$

The momentum, thermodynamic and moisture equations are

$$\frac{\partial u}{\partial t} = (f+\xi) v - \dot{\eta} \frac{\partial u}{\partial \eta} - \frac{R_d T_v}{a h_x} \frac{\partial \ln p}{\partial x} - \frac{1}{a h_x} \frac{\partial}{\partial x} (\phi + E) + P_u + K_u \tag{2.1.1.4}$$

$$\frac{\partial v}{\partial t} = -(f+\xi) u - \dot{\eta} \frac{\partial v}{\partial \eta} - \frac{R_d T_v}{a h_y} \frac{\partial \ln p}{\partial y} - \frac{1}{a h_y} \frac{\partial}{\partial y} (\phi + E) + P_v + K_v \tag{2.1.1.5}$$

where

$$\xi = \frac{1}{a h_x h_y} \left(\frac{\partial}{\partial x} (h_y v) - \frac{\partial}{\partial y} (h_x u) \right) \tag{2.1.1.6}$$

$$E = \frac{1}{2} (u^2 + v^2) \tag{2.1.1.7}$$

$$\frac{\partial T}{\partial t} = -\frac{u}{a h_x} \frac{\partial T}{\partial x} - \frac{v}{a h_y} \frac{\partial T}{\partial y} - \dot{\eta} \frac{\partial T}{\partial \eta} + \frac{\kappa T_v \omega}{(1 + (\delta - 1) q) p} + P_T + K_T \tag{2.1.1.8}$$

$$\frac{\partial q}{\partial t} = -\frac{u}{a h_x} \frac{\partial q}{\partial x} - \frac{v}{a h_y} \frac{\partial q}{\partial y} - \dot{\eta} \frac{\partial q}{\partial \eta} + P_q + K_q \tag{2.1.1.9}$$

The terms P_x and K_x represent tendencies from the physical parameterization and horizontal diffusion, respectively.

The hydrostatic equation takes the form

$$\frac{\partial \phi}{\partial \eta} = -\frac{R_d T_v}{p} \frac{\partial p}{\partial \eta} \tag{2.1.1.10}$$

and the continuity equation is

$$\frac{\partial}{\partial \eta} \frac{\partial p}{\partial t} + \nabla \cdot \left(\vec{v}_h \frac{\partial p}{\partial \eta} \right) + \frac{\partial}{\partial \eta} \left(\dot{\eta} \frac{\partial p}{\partial \eta} \right) = 0 \tag{2.1.1.11}$$

The definition of the divergence operator is

$$\nabla \cdot \vec{v}_h = \frac{1}{a h_x h_y} \left\{ \frac{\partial}{\partial x} (h_y u) + \frac{\partial}{\partial y} (h_x v) \right\} \tag{2.1.1.12}$$

By integrating the continuity equation, using the boundary conditions $\dot{\eta} = 0$ at $\eta = 0$ and $\eta = 1$, we obtain the equation for the surface pressure tendency

$$\frac{\partial p_s}{\partial t} = -\int_0^1 \nabla \left(\vec{v}_h \frac{\partial p}{\partial \eta} \right) d\eta \tag{2.1.1.13}$$

the equation for pressure vertical velocity

$$\omega = \frac{\partial p_s}{\partial t} + \int_\eta^1 \nabla \cdot \left(\vec{v}_h \frac{\partial p}{\partial \eta} \right) d\eta + \vec{v}_h \cdot \nabla p \tag{2.1.1.14}$$

and the equation for $\dot{\eta}$

$$\dot{\eta} \frac{\partial p}{\partial \eta} = \left(1 - \frac{\partial p}{\partial p_s} \right) \frac{\partial p_s}{\partial t} + \int_\eta^1 \nabla \cdot \left(\vec{v}_h \frac{\partial p}{\partial \eta} \right) d\eta \tag{2.1.1.15}$$

Finite difference formulations

The vertical staggering of the variables, with temperature, wind components and humidity at the model "full" levels and geopotential and vertical velocities at the model "half" levels, is the same as used in the present ECMWF model and this is the case also for the vertical finite differencing scheme. The horizontal differencing scheme is similar to that used in the previous ECMWF grid-point model (Arakawa 1966 and Sadourny 1975).

Time integration scheme

A three time level semi-implicit time stepping scheme is used in the HIRLAM model. The time stepping is done by first computing explicit new values at time $t+\Delta t$ using a leapfrog scheme for the dynamic terms and a forward scheme for the remaining terms (some processes such as vertical diffusion are using implicit techniques). Then the implicit correction terms are added to the explicitly calculated values at the new time-step. Further, the values at the new time-step are relaxed toward the prescribed boundary values (Kållberg and Gibson 1977) and finally these new values at time $t+\Delta t$ are time-filtered. The semi-implicit formulation follows Simmons and Burridge (1981) and is based on linearization around a constant basic temperature (300 K) and a constant basic surface pressure (800 hPa). The model may also be integrated using an explicit time scheme.

2.1.2 Physical parameterization schemes.

Horizontal diffusion

The horizontal diffusion affects the horizontal wind components, temperature and specific humidity. The standard horizontal diffusion in the model is a non-linear second order scheme. An option exists to utilize a linear fourth order scheme. For temperature, the fourth order scheme is formulated such that the diffusion is carried out approximately along pressure surfaces. This special treatment of temperature was introduced in order to prevent a tendency for spurious heating over mountain tops, which results from diffusion of temperature along model surfaces. This heating in turn may lead to spurious convection and precipitation. For specific humidity, a height dependent diffusion coefficient, with a maximum value around the jet-stream level, is used in the non-linear second order scheme.

Vertical diffusion.

The vertical diffusion scheme affects the horizontal wind components, dry static energy and specific humidity. Surface fluxes affect the prognostic values in the lowest model layer. They are determined by means of a drag coefficient formulation, using Monin-Obukov similarity theory for the atmospheric surface layer. The drag coefficients are functions of static stability and a roughness length. For each gridpoint a fraction of land and a fraction of sea ice are defined. The roughness length over the fraction of the grid area covered by open sea is computed by the Charnock's formula while the roughness lengths over land and ice are constant in time. The roughness length over land is given as a combination of a contribution from vegetation and a contribution from the sub-grid scale variation of orography. For ice covered sea a small value of the roughness length (0.001 m, probably too small) is used. For each gridpoint the surface fluxes are computed separately over land including ice covered part of the sea and over open sea, including lakes. The distinction between "land plus sea ice" and "open sea" applies only to the surface fluxes and not to the fluxes above the lowest model level.

The calculation of fluxes above the lowest model level is based on a mixing length formulation, using exchange coefficients, which depend on static stability. The static stability is described by means of a Richardson number. The analytic formulae describing the dependency of drag/exchange-coefficients on static stability are those proposed by Louis et al. (1981). The effect of shallow convection is included by defining a modified Richardson number.

Convection

A Kuo-type of scheme is used: layers taking part in the convection are defined by demanding that an air parcel lifted from one model layer to the next is positively buoyant and becomes saturated. The transition from positive to negative buoyancy marks the upper limit of the convective layers. It is further demanded that the vertically integrated moisture convergence is positive. The scheme allows for more than one set of convective layers. A partitioning parameter, which is determined from the relative humidity in the convective layers, defines the fraction of total moisture convergence remaining in the atmosphere. The rest is released as precipitation. Below convective layers evaporation of precipitation occurs ("Kessler" type of evaporation parameterization). Freezing/melting of precipitation is neglected. The precipitation at the ground is assumed to be snow if the temperature at the lowest model layer is below 0 degree C, otherwise it is assumed to be rain.

Stratiform condensation.

The condensation process is defined by demanding that the grid box specific humidity should not exceed a saturation value, which optionally can be chosen to be less than the true saturation specific humidity. The amount of moisture, which is condensed in order to restore saturation (a first order adjustment) is released as precipitation, and temperature is affected by the corresponding heat release. The evaporation of stratiform precipitation and the distinction between rain and snow are done in the same way as for convective precipitation.

Radiation.

A new radiation scheme was designed for the HIRLAM model. The heating/cooling rate is expressed as the sum of a "cloudy" contribution and a "clear air" contribution. This applies to both short- and longwave radiation. Any model layer may contain clouds, which are diagnosed from relative humidity.

The transmission of shortwave radiation through the atmosphere is affected by scattering and absorption. The scheme distinguishes between direct and diffuse solar radiation. A diurnal variation of the solar zenith angle is included. The atmospheric absorption- and scattering properties as a function of wavelength are parameterized in terms of humidity and density. The reflectance of clouds depends on cloud type, cloud depth and solar zenith angle. Multiple scattering between model layers affects the transmission and absorption of solar radiation. The shortwave albedo of the ground depends on geographical position, a diagnostic snow cover and the solar zenith angle.

The longwave clear air cooling is a "direct cooling to space" formulation (London and Sasamori(1968)), which is improved by defining a modified cooling/heating below clouds and by a dependency of clear air cooling on temperature curvature. The cloudy contribution to heating/cooling rate and the net longwave radiation at the ground are defined by means of simple emissivity methods. The emissivity of clouds depends on cloud type and cloud depth, which are defined in terms of the vertical hybrid coordinate.

Surface processes.

The surface parameterization scheme used in the present HIRLAM Level 1 model is in essence the previous ECMWF scheme with three soil layers. The ECMWF scheme has been modified with special attention paid to the treatment of snow and sea ice. The scheme describes the evolution of soil temperature, soil water content and snow depth over land/ice by means of simple prognostic equations. Ice covered sea is treated as land. No calculations are done over open sea where the temperature field is kept constant during the model integration. Temperature and soil water content are predicted in the two upper layers, while climatological values are used in the lowest layer. Soil temperature of the uppermost soil layer is affected by the net heat flux at the ground as a result of net radiation, sensible and latent heat fluxes. It is also affected by ground heat conduction. The heat diffusivity of the upper soil layer is a decreasing function of a diagnostic snow cover determined from snow depth. Over "fraction of land" the surface temperature is allowed to increase above 0 degrees C before all snow has melted.

The soil water content of the uppermost layer is affected by evaporation over the fraction of the grid area without snow cover. It is further influenced by the precipitation in the form of rain, snow melt and ground conduction of soil water. Temperature and soil water content of the intermediate layer are influenced by ground conduction of heat and moisture, respectively. If the soil water content in any of the soil layers exceeds a critical value, runoff of the excessive moisture is assumed to take place. Snow depth is controlled by snow fall from the atmosphere, sublimation from the snow-covered fraction of the grid area and melting of snow.

2.2 The non-linear normal mode initialization scheme.

The HIRLAM level 1 initialization scheme is a nonlinear normal mode scheme utilizing the nonlinear balance condition and the iterative procedure used to achieve this balance as proposed by Machenhauer (1977). The form of this iteration scheme actually used is that introduced by Andersen (1977), in which tendencies determined by an Eulerian time step with the forecast model are utilized. As an additional condition needed to compute the initialization increments of temperature and surface pressure we use the linear condition proposed by Machenhauer in Andersen (1977).

In the standard version all gravity modes in the four gravest vertical modes are initialized using adiabatic tendencies and two iterations. The vertical modes are determined as eigenfunctions to a linearized form of the vertically discretized forecast model. The linearization is performed with respect to a dry basic state at rest with a constant temperature in each of the model levels determined from the ICAO standard atmosphere. The horizontal modes are eigenfunctions in terms of velocity potential, stream function and geopotential perturbations of linearized shallow water systems of equations with equivalent mean depths determined by the vertical eigenvalue problem. In the linearized system a constant Coriolis parameter is used, its value is that at the center of the limited area.

The linearized shallow water systems are discretized on the mass points of the rotated lat-long grid of the prediction model using the usual second order finite difference approximation for the Laplace operator. As this discretization is not strictly consistent with that used in the prediction model a proper balancing of the smallest scales is not ensured by the initialization steps. The horizontal diffusion and the Asselin time filter in the model should, however, take care of the damping of any high frequency gravity oscillations in these smallest scales.

The horizontal structures of the normal modes are given by discrete harmonics which are the eigenfunctions of the discrete Laplace operator and satisfying the Dirichlet boundary conditions, i.e. which are zero at the boundaries of the limited area. Note that in the initialization procedure only the gravity

mode tendencies are represented by these horizontal structure functions. Therefore, if these tendencies were large at the interior points next to the boundaries, the resulting initialization increments would include large amplitude, small scale components due to the fact that the normal modes are zero at the boundaries. To avoid such small scale increments, geostrophically balanced boundary conditions are used when computing the tendencies of the velocity potential and stream function, needed in the initialization, from the tendencies of velocity components, determined by the prediction model.

The tendencies computed from the model and used in the initialization steps include contributions from the boundary fields through the boundary relaxation scheme of the prediction model. Thus the forcing due to this boundary relaxation is taken into account together with the nonlinear forcing in the initialization. To avoid unrealistically small scale initialization increments due to the boundary relaxation it is essential that the boundary (or background) fields are well balanced. Furthermore small contributions from the background fields to the tendencies in the boundary zone are ensured by the assumed linear variation in time of these fields over relatively large time intervals (the standard interval is 6 hours).

For the initialization code we have used as a starting point an early version of a KNMI nonlinear normal mode initialization program developed by Bijlsma and Hafkenscheid (1984).

2.3 The analysis scheme.

The HIRLAM Level 1 analysis scheme for wind, mass and humidity fields is a limited area version of the ECMWF analysis scheme. The basic technique of the ECMWF scheme is optimum interpolation (Gandin 1963) extended to multivariate three-dimensional interpolation of observed deviations from forecast first guess fields (Lorenc 1981). Analyzed parameters are geopotential, wind components and relative humidity. Analysis increments are evaluated directly on the forecast model levels. In addition to the general analysis scheme for wind, mass and humidity, a separate analysis scheme for sea surface temperature and sea ice coverage has been developed. This analysis scheme is based on the successive correction technique.

3. Operational experiences with the HIRLAM Level 1 system

3.1 FMI experiences.

The Finnish Meteorological Institute (FMI) started their operational production of HIRLAM forecasts in January 1990. Besides optimization for the particular computer configuration, a Cray XMP-4 shared with the Finnish State Computing Centre, the FMI HIRLAM system is very close to the standard HIRLAM Level 1 system described above. The integration area consists of 130 * 100 horizontal gridpoints (see Figure 1), the horizontal resolution is 0.5 * 0.5 degree and the number of vertical levels is 16.

The operational introduction of the HIRLAM system at FMI in January went very smoothly and there have been very few breaks in the operational production since then. One problem has been the poor availability of TEMP SHIP data in the FMI data base used by the HIRLAM data assimilation, but this problem turned out to be related to the FMI telecommunication system. After the introduction of a new telecommunication system at FMI, the problem disappeared. The acceptance of the FMI HIRLAM products by the FMI forecasters has been very good. This is certainly due to the good quality of the forecasts, at least with regard to the traditional synoptic scale output products. This high quality is confirmed also by objective verification scores and in comparison with corresponding scores for e.g. ECMWF forecasts. Figure 2 shows a map of the mean errors and Figure 3 a map of the RMS errors of the 500 hPa height forecasts for the period June to August 1990. The FMI verification scores are averages over all four (00, 06, 12 and 18 UTC) forecast runs. The inclusion of the 06 and 18 UTC forecasts puts

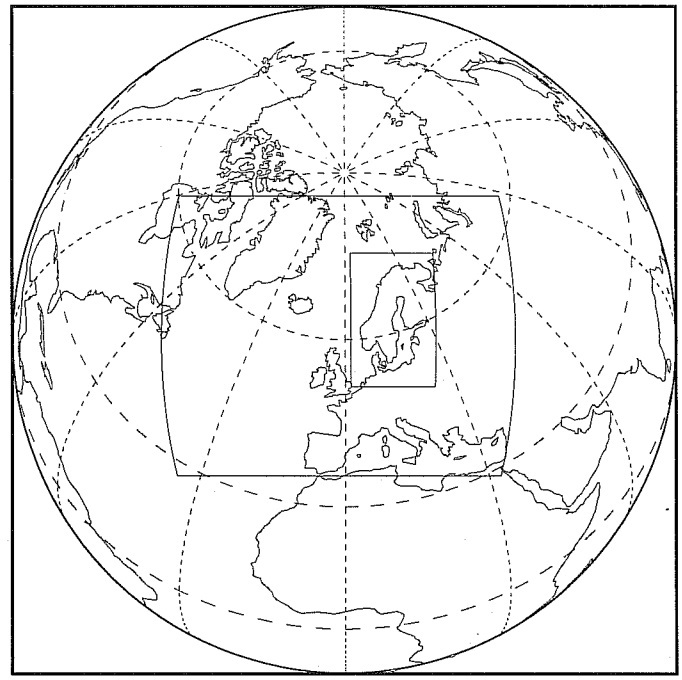

Figure 1: FMI HIRLAM integration area.

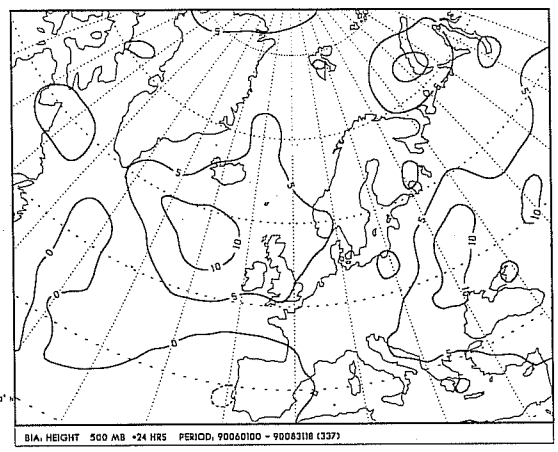

Figure 2: FMI HIRLAM +24h 500 hPa height mean forecast error. June-August 1990.

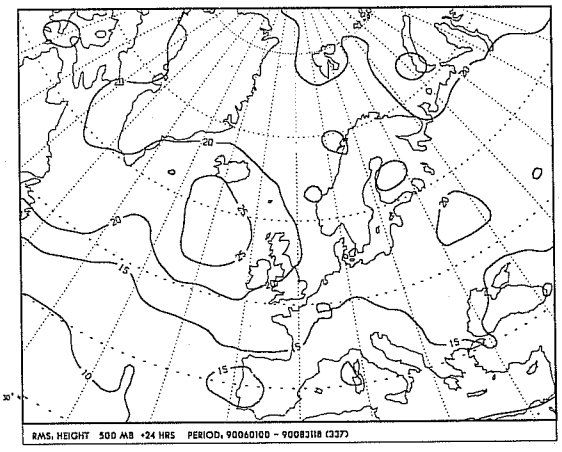

Figure 3: FMI HIRLAM +24h 500 hPa height RMS forecast error. June-August 1990.

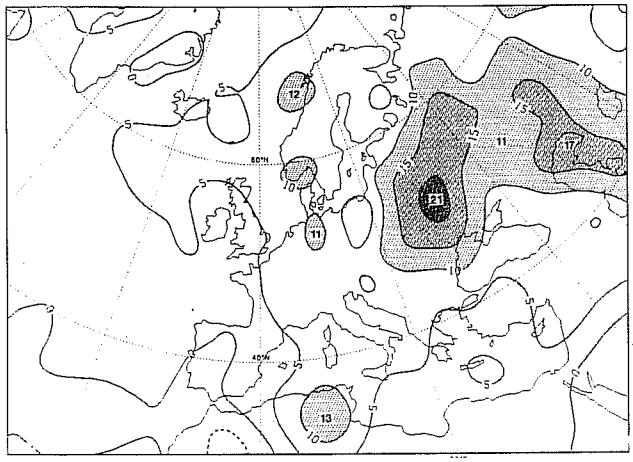

Figure 4: ECMWF +24h 500 hPa height mean forecast error. June-August 1990.

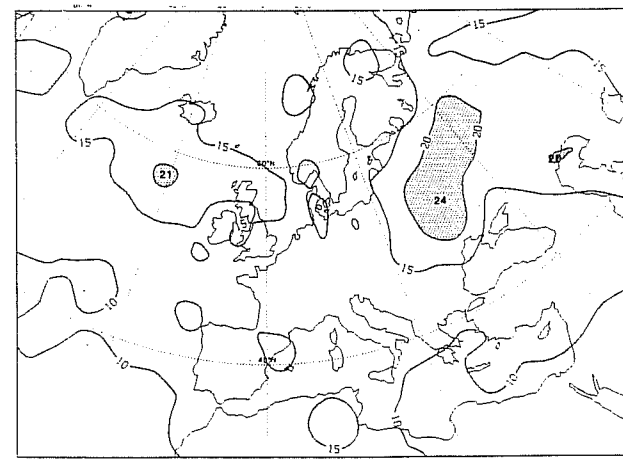

Figure 5: ECMWF +24h 500 hPa height RMS forecast error. June-August 1990.

the FMI forecasts at slight disadvantage to the ECMWF forecasts. Corresponding maps for the ECMWF forecasts are shown in figures 4 and 5. The HIRLAM mean errors are slightly smaller than the corresponding ECMWF errors. As regards the RMS errors, the HIRLAM errors have the same magnitude as the ECMWF errors over the European land areas, while the HIRLAM errors are significantly larger in the baroclinically active zone over the North Atlantic south of Greenland. Obviously these larger errors are related to the use of too old boundary values in the operational FMI HIRLAM runs - the 12 UTC FMI HIRLAM forecasts runs start with 24 hour old ECMWF forecasts on the lateral boundaries.

The dependency of the forecast quality on the age of the lateral boundary conditions is clearly illustrated by comparing verification scores valid at 12UTC and 00UTC respectively, see figures 6 and 7 including verification scores for the summer 1990. At 12 UTC, the +48 h forecasts, based on 12UTC initial data and old boundaries, are relatively worse than +36 h forecasts, based on 00UTC initial data and fresh boundaries, as compared to verification at 00UTC where the +48 h forecast is based on fresh boundaries and the +36 forecast is based on old boundaries. The difference in forecast quality is, however, not always as clear as during the summer 1990, and it certainly depends on the prevailing circulation type. At least in June 1990, the circulation was dominated be strong fast flow over the western boundary of the integration area. During the winter 1990-91 the same effect was not as pronounced as during the period illustrated above.

FMI are producing HIRLAM forecasts 4 times a day with initial data at 00UTC, 06UTC, 12UTC and 18UTC. The main data source at 06UTC and 18UTC are single level data like surface data and aircraft data. Only a few radiosonde observations are made at 18 UTC and the analysis at that time is to a large extent a first guess. Very little difference is therefore seen between the 12 and 18 UTC forecasts. The verification scores in figures 8 and 9 indicate, however, that the data assimilation and forecast system manages to extract useful information from the single level data at 06 UTC since e.g. the + 30 h forecasts based on 06UTC data have significantly better mean verification scores than the +36 h forecasts from 00UTC data (the lateral boundaries for 00UTC and 06UTC forecasts are the same).

It is also of general interest to investigate to what extent the data assimilation manages to extract information from the observational data. RMS deviations of radiosonde observations from 6 h forecasts (analysis first guess), un-initialized analysis fields and initialized analysis fields for the winter 1990-91 are given in figures 10 and 11. The analysis first guess RMS deviation in the middle troposphere of 4 m/s is reduced to 2 m/s by the analysis and very little is lost by the initialization for the wind field. Thus the analysis/initialization cycle accepts the wind observations very well, while during the initialization some part of the height field information is lost due to adjustment towards the wind data.

The most serious problem with the FMI operational HIRLAM forecasts is a systematic cold bias in the low level temperature forecasts. Figure 14 clearly shows the evolution of this bias of the 850 hPa temperature error as a function of forecast length. This bias of the forecast error is present in all seasons. The low level temperature errors depend on the synoptic situation and this is clearly illustrated by looking at spatial correlations of the 850 hPa height error, Figure 12. These correlations have a much stronger large scale components as compared to the analysis correlation functions derived for ECMWF forecast errors and used by the HIRLAM analysis scheme as well as compared with correlations at higher levels, Figure 13. Some efforts have been spent on the problem to find the source of the low level systematic errors. Some trials to modify parameters of the parameterization schemes for e.g. vertical diffusion, surface evaporation and convective condensation have so far had a limited success. Some minor improvements were found by introduction of an analysis of sea ice and sea surface temperature at FMI. The poor vertical resolution of the 16 level version of the HIRLAM forecast model is another likely cause of the problem.

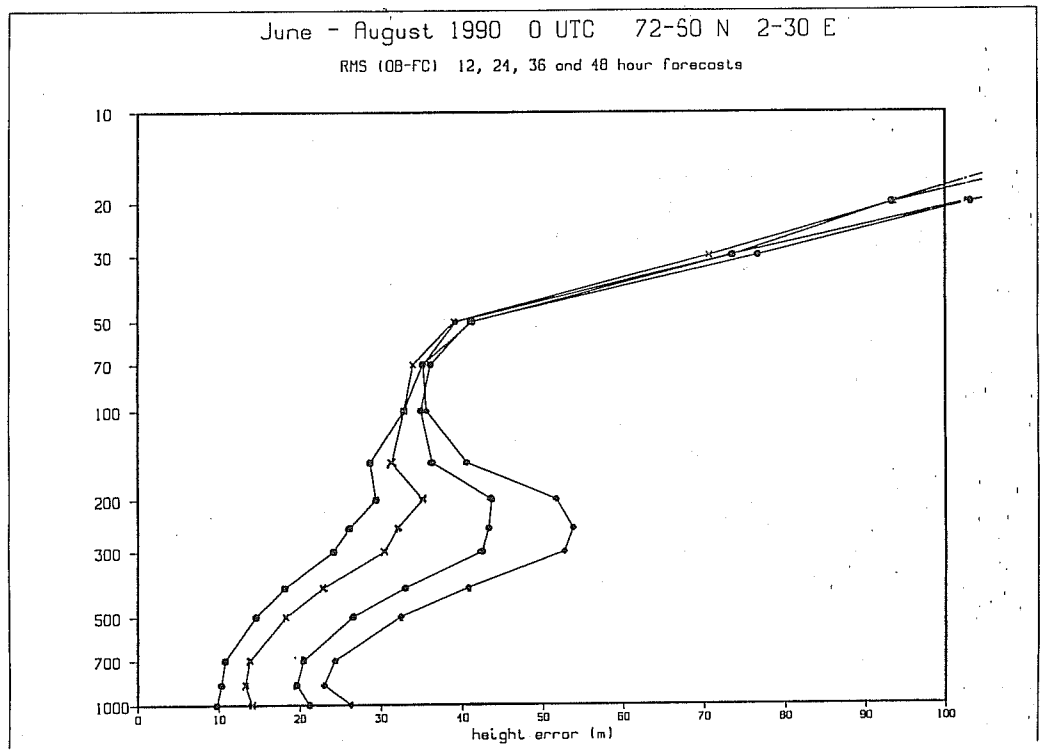

Figure 6: FMI HIRLAM height RMS forecast errors as verified against 00UTC radiosonde data. +12h, +24h, +36h and +48h. June - August 1990.

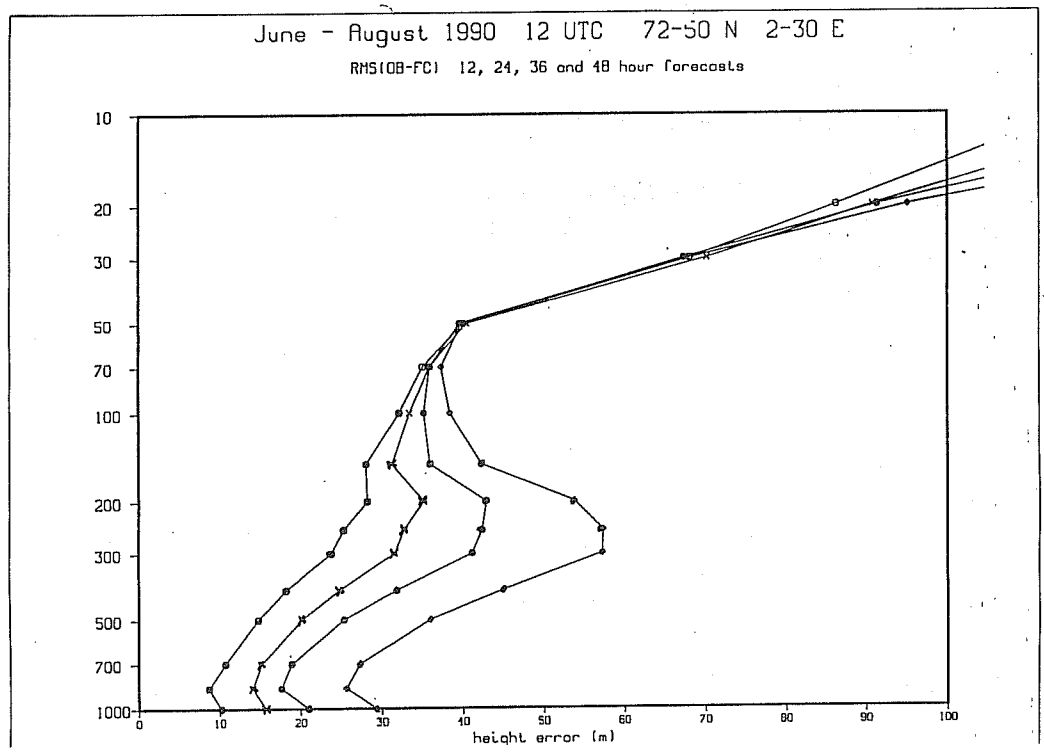

Figure 7: FMI HIRLAM height RMS forecast errors as verified against 12UTC radiosonde data. +12h, +24h, +36h and +48h. June - August 1990.

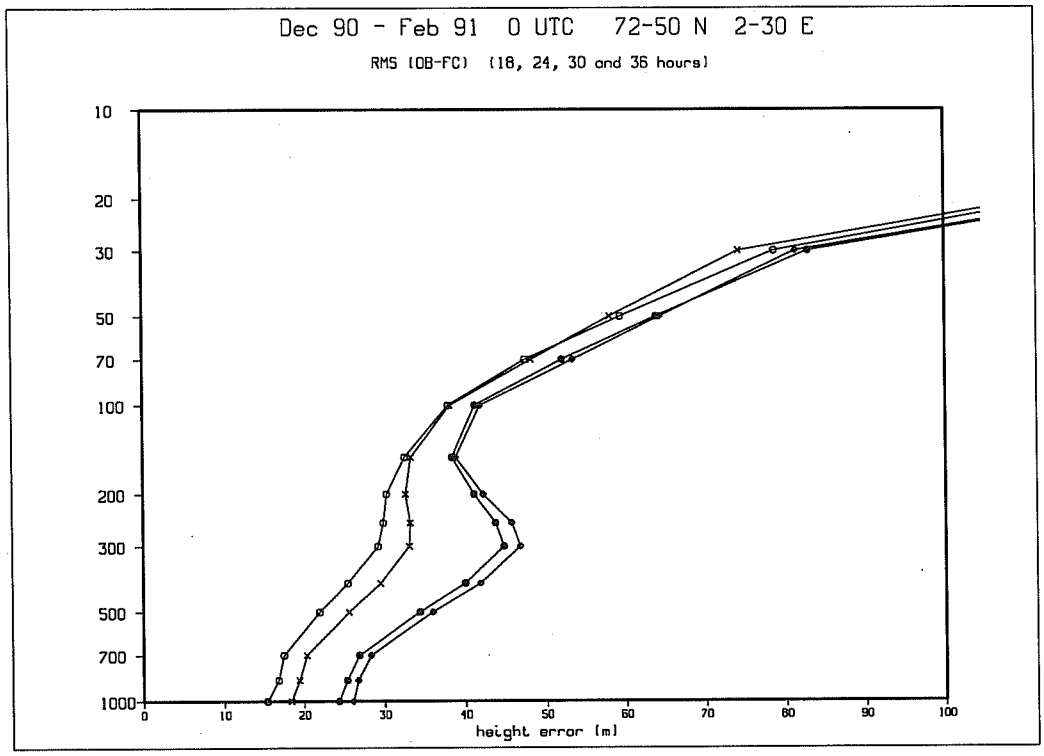

Figure 8: FMI HIRLAM height RMS forecast errors as verified against 00UTC radiosonde data. +18h, +24h, +30h and +36h. December 1990 - February 1991.

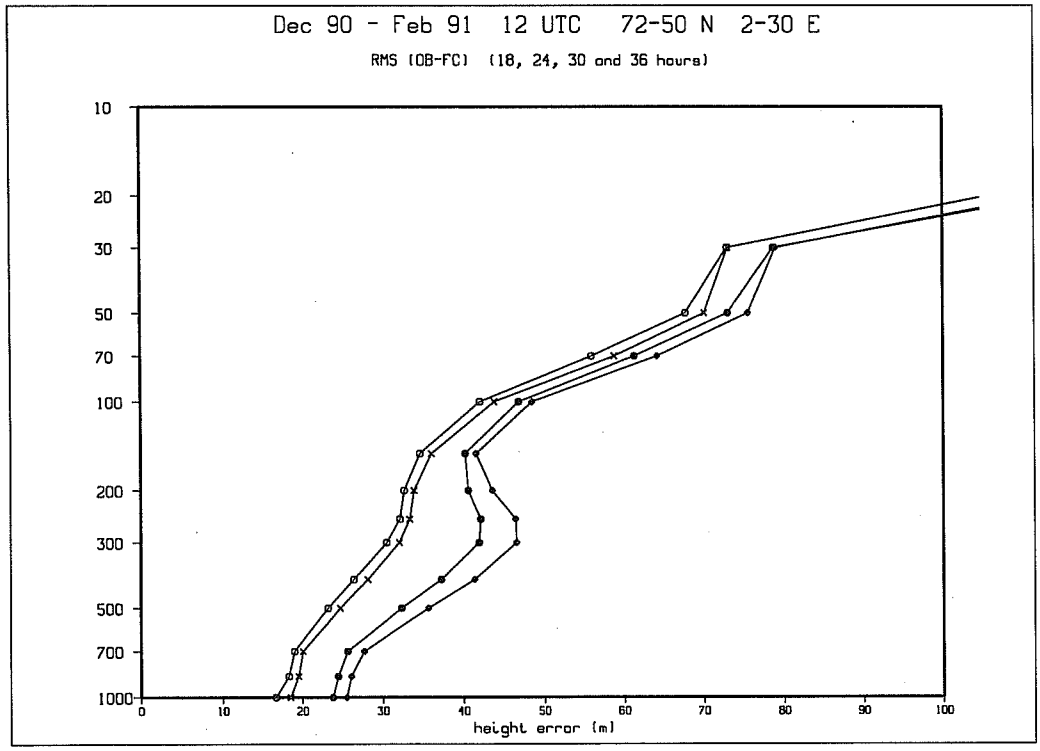

Figure 9: FMI HIRLAM height RMS forecast errors as verified against 12UTC radiosonde data. +18h, +24h, +30h and +36h. December 1990 - February 1991.

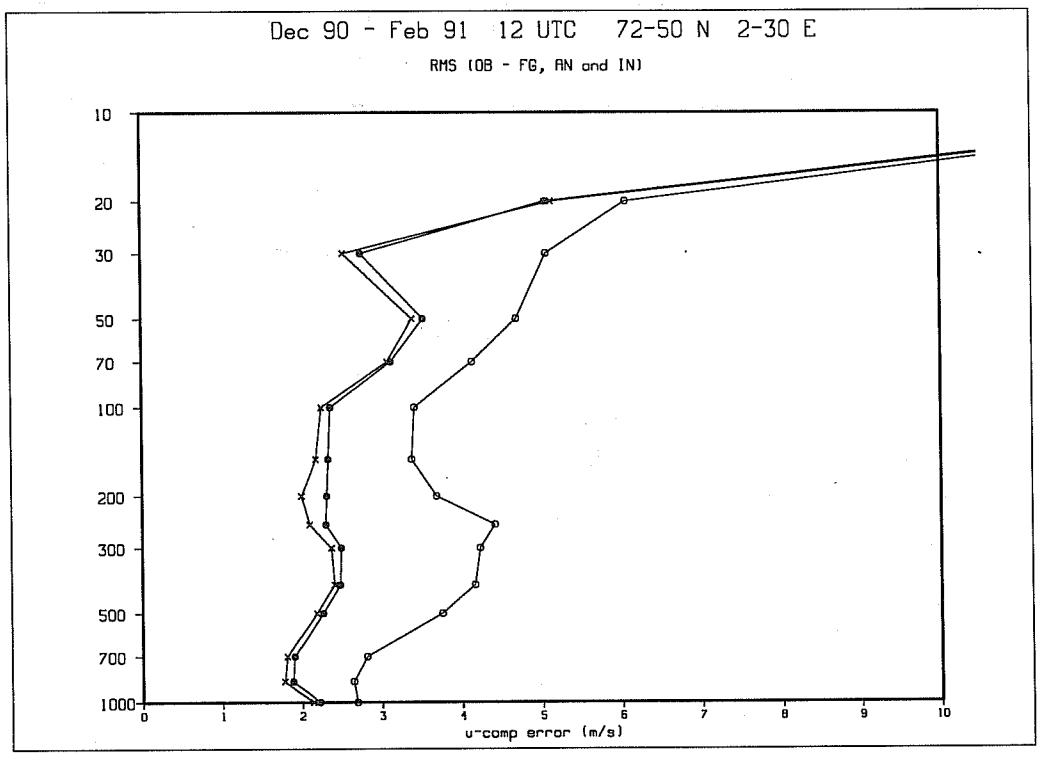

Figure 10: RMS U component differences between radiosonde data and FMI HIRLAM (1) +6h forecasts, (2) Un-initialized analyses (3) Initialized analyses. December 1990 - February 1991.

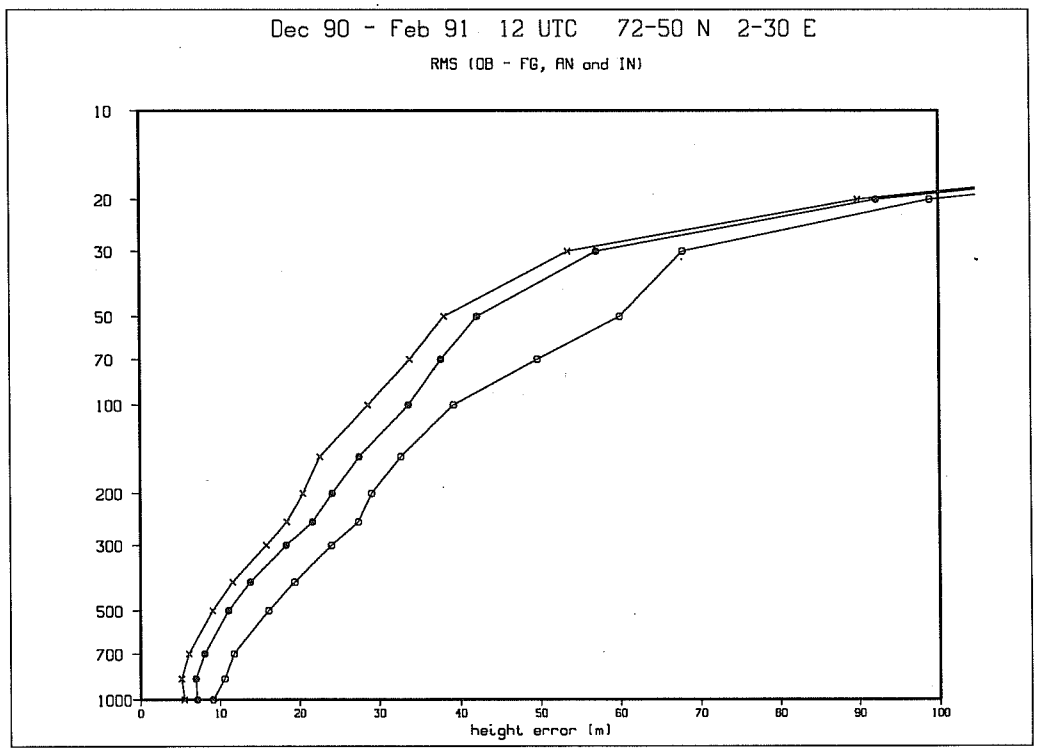

Figure 11: RMS height differences between radiosonde data and FMI HIRLAM (1) +6h forecasts, (2) Un-initialized analyses (3) Initialized analyses. December 1990 - February 1991.

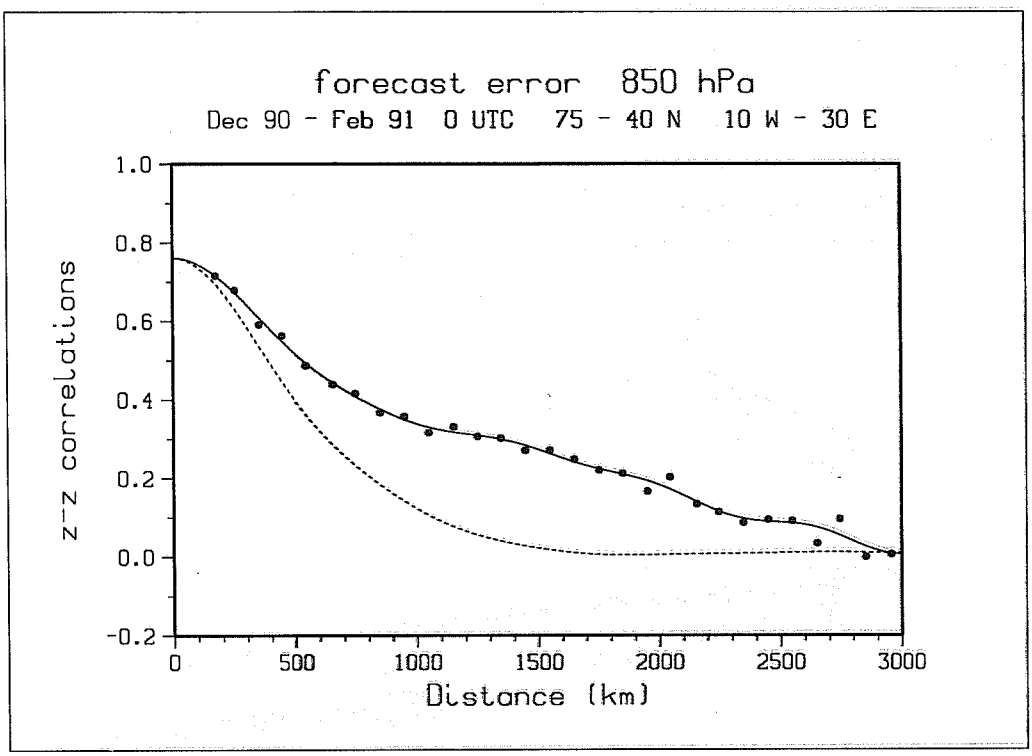

Figure 12: Horizontal forecast error correlations derived from FMI HIRLAM 850 hPa height forecasts and radiosonde data. December 1990 - February 1991. Dotted curve represents correlation function used in the analysis.

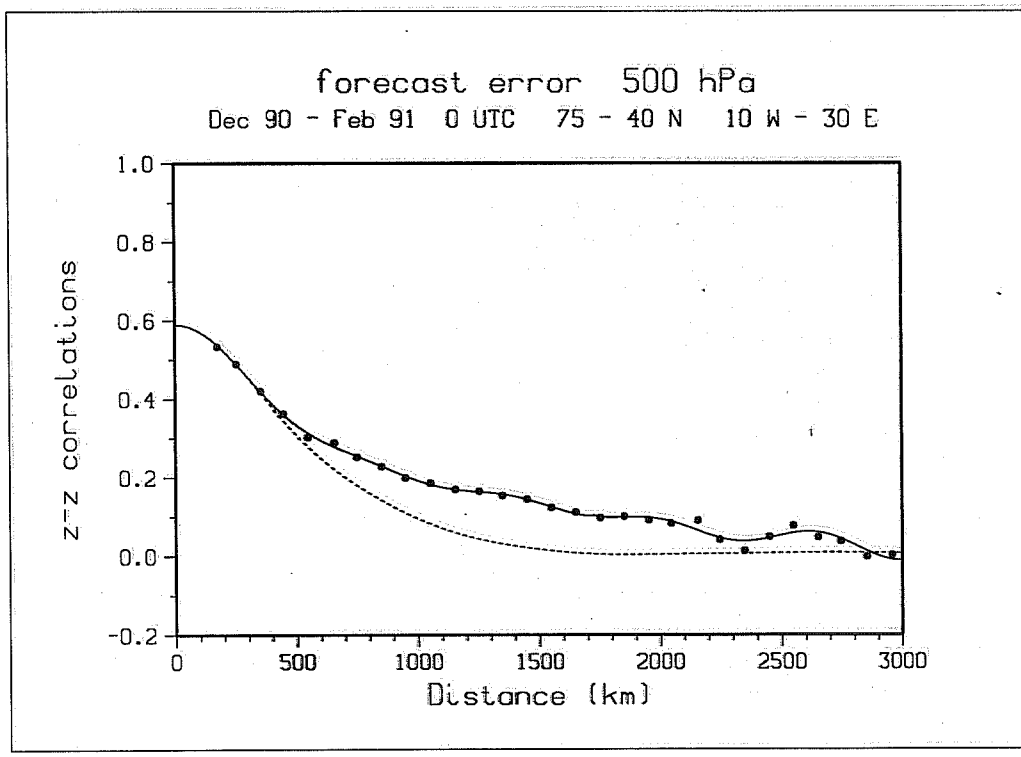

Figure 13: Horizontal forecast error correlations derived from FMI HIRLAM 500 hPa height forecasts and radiosonde data. December 1990 - February 1991. Dotted curve represents correlation function used in the analysis.

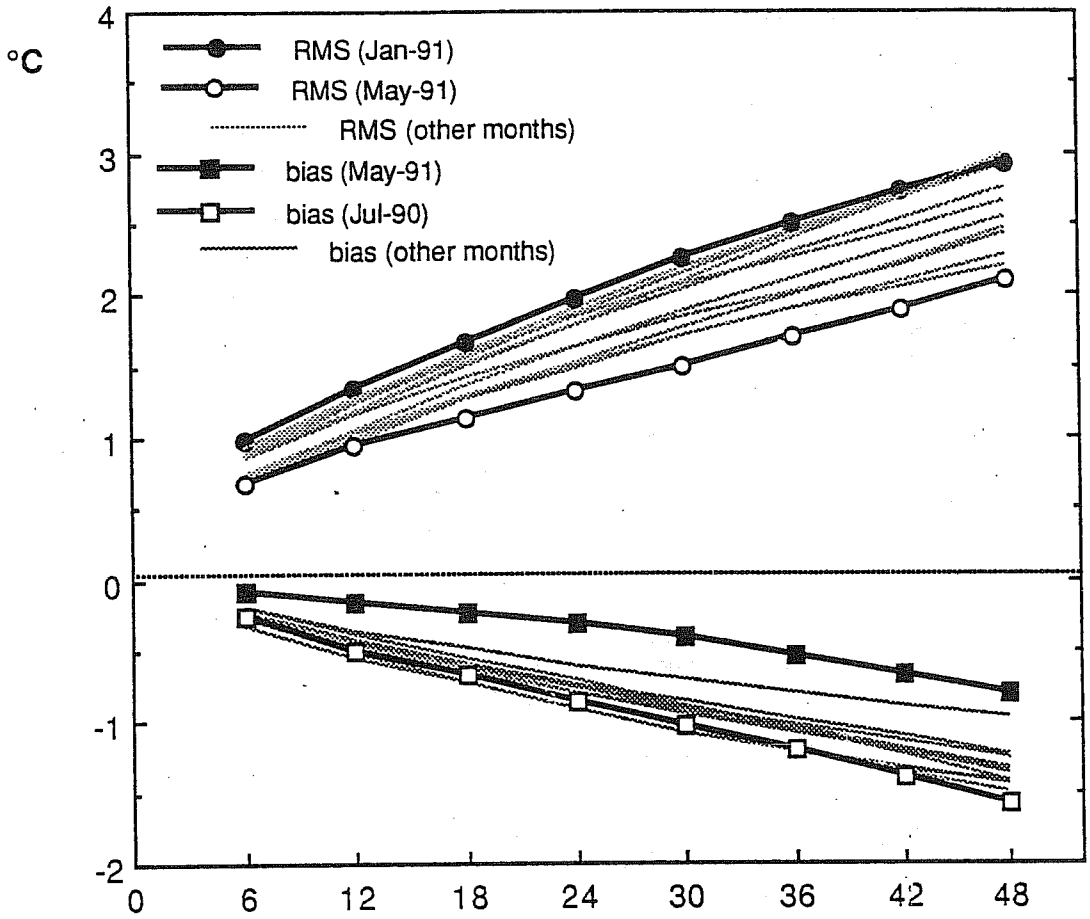

Figure 14: Summary of monthly mean FMI HIRLAM 850 hPa temperature forecast errors. June 1990 - May 1991.

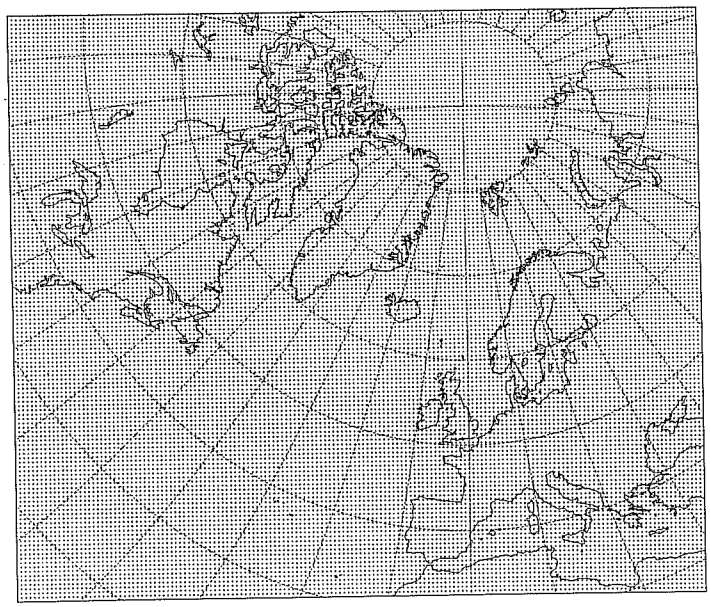

Figure 15: DMI GR-HIRLAM integration area.

3.2 DMI experiences.

The Danish Meteorological Institute has been running the HIRLAM Level 1 system on a CONVEX C-220 computer system since November 1990. Recently a 4-processor Convex C-240 was installed and from next year a much more powerful computer in the CONVEX C3 series will be utilized. The DMI version of the HIRLAM system differs from the standard Level 1 system mainly in the design of the timestepping of the model. Physical tendencies are calculated each third timestep only and this has made it possible for DMI to run on a rather large area, GR-HIRLAM with 162*136 gridpoints with a horizontal resolution of 0.51*0.51 degrees and 16 vertical levels - see figure 15. The large area run is supplemented with a smaller area run (DK-HIRLAM] which is run with boundary values from the larger area run and with a shorter cut-off time for the observations. With the exception for some initial problems with pre-processing of observations, also the implementation of the HIRLAM system at DMI went smoothly.

Verification against observations during the winter 1990-91 indicated a forecast quality that was better or at least as good as the quality of the UKMO limited area forecasts (see Figure 16 for mean sea level pressure). This quality of the DMI HIRLAM forecasts has gradually increased the credibility of the DMI numerical forecasts among the forecasting office staff of DMI (the credibility of the national NWP products was once a problem at DMI as it also is at many other weather services with limited staff and computer resources for NWP). Verification from the summer months of 1991 indicated that the UKMO Limited area model runs has caught up in quality with the DMI forecasts and that the ECMWF forecasts still are better for forecast lengths beyond 12 hours (Figure 17).

The DMI low level temperature forecasts suffer from a similar cold bias as the FMI HIRLAM forecasts, see Figure 18. The significant positive bias of the DMI 850 hPa initial temperature field may be explained by a too stable and too cold first guess forecast that is only corrected for by the layer mean temperature between the surface and 850 hPa.

3.3 Subjective evaluation of operational HIRLAM forecasts at SMHI

The Swedish Meteorological and Hydrological Institute will not have the computer resources to apply the HIRLAM system operationally until spring 1992. With the emphasis to familiarize the forecasters with the HIRLAM forecasts and also to participate in the assessment of the quality of the HIRLAM forecast products, SMHI has received HIRLAM forecast maps from FMI and DMI during a few periods. These forecasts have been evaluated subjectively and compared to "old" SMHI LAM model results as well as with the UKMO LAM forecasts. Figure 19 contains a summary of mean values of subjective scores for 77 cases during October 1990 - January 1991. The following scale of scores was used: 5 = excellent, 4 = good, 3 = useful, 2 = bad and 1 = poor. It can be seen that the FMI HIRLAM forecasts were given very good scores during the period. The quality difference between the UKMO and the FMI forecasts at +36h is significant at the 1% level.

A second subjective evaluation was carried out in May 1991. Forecast from DNMI and Meteo France as well as DMI and FMI HIRLAM forecasts were received and evaluated during this period. The general quality of the synoptic scale forecasts for sea-level pressure etc. for the Northern European area was considered excellent for all the forecasts during the actual period and mean values of the subjective scores did not indicate any significant difference between the forecasts. Since it was not appropriate to evaluate the Meteo France PERIDOT forecasts over the Northern European area (the northern boundary of PERIDOT goes through southern Sweden) a special evaluation was carried out for a mid-western European area. Mean subjective scores for this May period are contained in the table below. Note the good scores for the Meteo France PERIDOT forecasts.

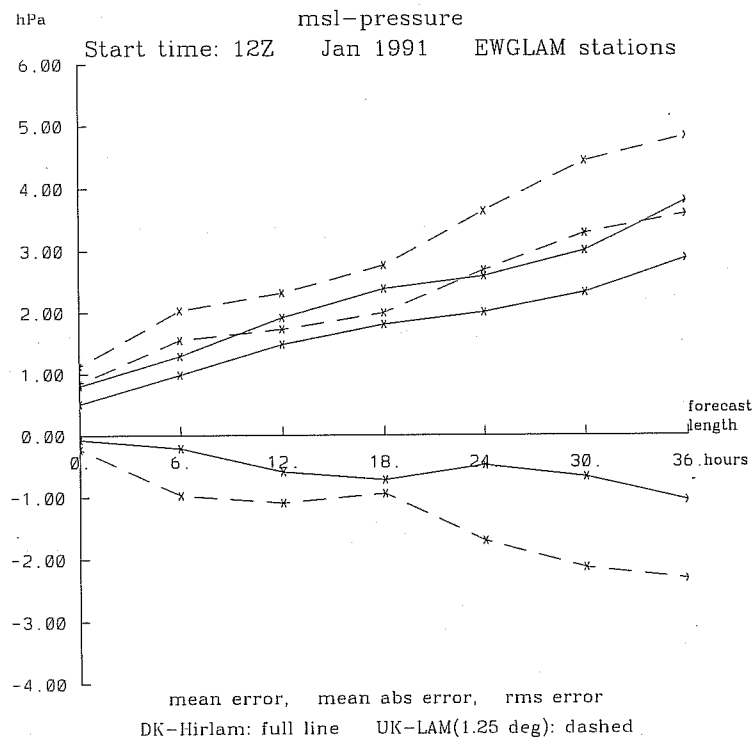

Figure 16: Verification of DMI HIRLAM(full line) and UKMO LAM(dashed line) 12 UTC sea-level pressure forecasts against surface data. Mean error, mean abs.error and RMS error. January 1991.

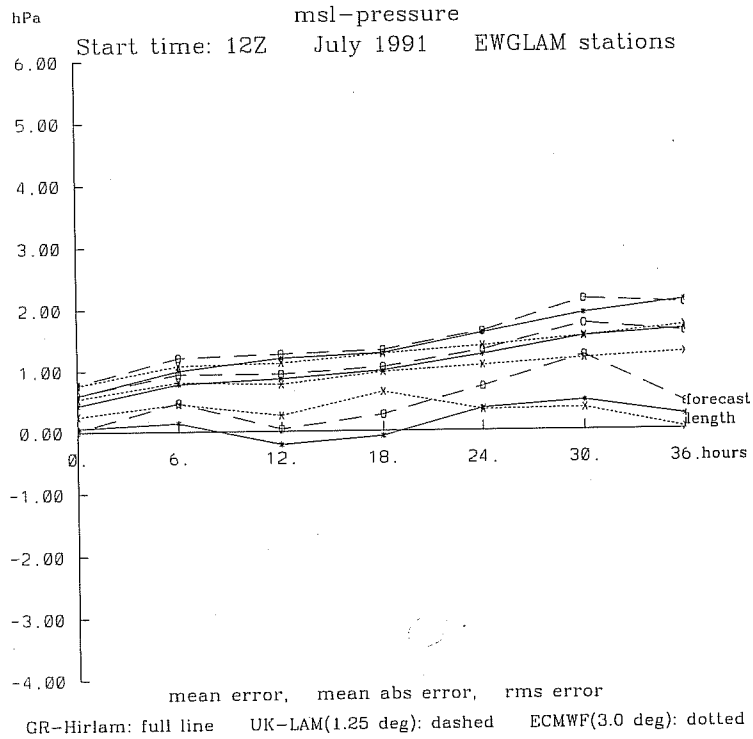

Figure 17: Verification of DMI HIRLAM(full line), UKMO LAM(dashed line) and ECMWF(dotted line) 12 UTC sea-level pressure forecasts against surface data. Mean error, mean abs.error and RMS error. July 1991.

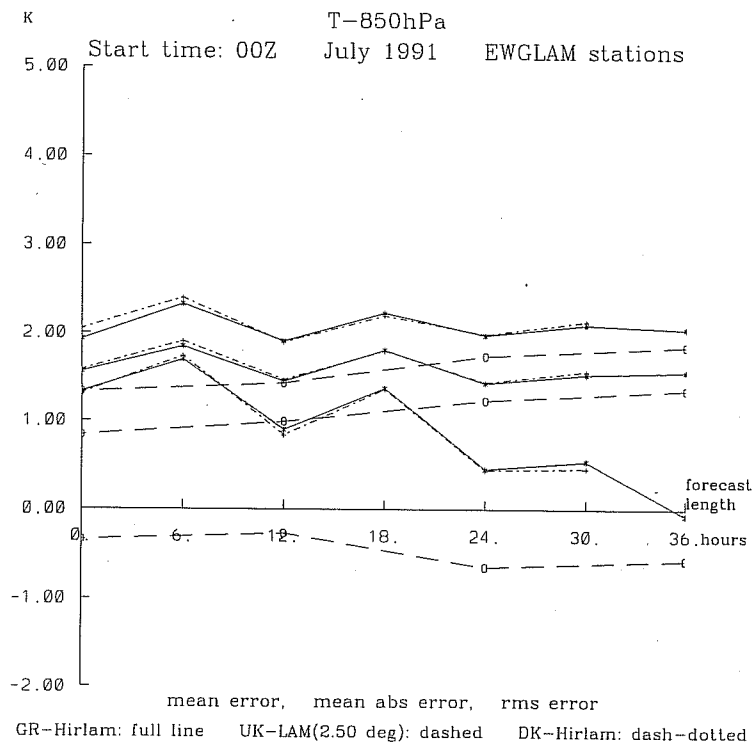

Figure 18: Verification of DMI HIRLAM(full line), UKMO LAM(dashed line) and ECMWF(dotted line) 12 UTC 850 hPa temperature forecasts against radiosonde data. Mean error, mean abs.error and RMS error. July 1991.

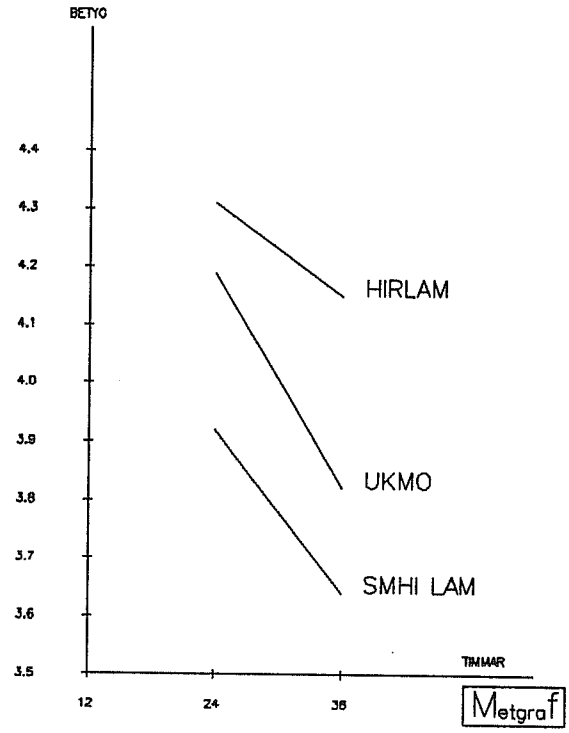

Figure 19: Average subjective verification scores (see text).

Model	+24h	+36h
UKMO LAM	4.39	4.12
DMI HIRLAM	4.51	4.25
PERIDOT	4.57	4.25
ECMWF	4.41	4.13

4. HIRLAM 2 research activities

The HIRLAM 2 research program covers a wide range of activities, most of which are related to improvements of the HIRLAM forecasting system and to development of new system components. Here, only a few examples of these activities will be reviewed.

4.1 Meso-scale forecast experiments

In order to explore the behavior of the HIRLAM model in high resolutions, series of mesoscale forecast experiments have been run by the different HIRLAM groups. Here the experiments carried out by the SMHI group will be reviewed. The second case study to be presented, the "Baltic Bomb", was carried out by Per Kållberg SMHI.

4.1.1 A case study of a cold air outbreak over the Baltic Sea, 12 January 1987

Heavy snowfall along the Swedish east coast during winter situations with persistent easterly flow are often associated with mesoscale convection bands over the Baltic Sea. These snowfalls cause traffic hazards and communication problems. A proper understanding and forecasting of these events are considered essential. By the use of radar and satellite data, these snowbands have recently been studied by Andersson and Nilsson (1990). One of their cases, 12 January 1987, was selected as a test case for running the HIRLAM model with different horizontal resolutions (grid lengths 22 km and 55 km) as well as with different model formulations and different initial data.

The weather situation for the case study is illustrated by the NOAA-10 IR satellite image for 12 January 1987 18:11 UTC in Figure 20. Very cold air, as low as -30 C at the surface, was situated over the North-eastern part of the European continent. The air flow over the Nordic area was dominated by north-easterly winds. Mesoscale convection bands were formed over the ice-free areas of the Baltic Sea, and these bands were particularly strong along trajectories starting over the Gulf of Finland and ending over the Swedish east coast. Also notice the lack of clouds (and convection) in a small area close to the Swedish east-coast north of the strongest convection bands. This geographical distribution of convective precipitation, confirmed by measurements from the SMHI radar in Norrköping, is very typical during winter-time situations with north-easterly flow of cold air over the (warmer) Baltic Sea. Besides the convection bands over the central parts of the Baltic Sea, also notice the strong convection over the Bay of Riga and over the Sea of Kattegatt and the North Sea.

Some forecast experiments for this particular case study were carried out with a horizontal resolution of 0.5 degree. Forecast maps from these experiments will not be shown here but the main conclusions from these low resolution experiments may be summarized as follows:
- The model is able to predict precipitation in areas where precipitation is observed. The relatively coarse horizontal resolution compared to the geometry and dimensions of the Baltic Sea, does not permit a detailed description, however, of the convective bands.
- The forecast was very sensitive to the selection of the horizontal diffusion scheme. With the second order non-linear horizontal diffusion scheme, the precipitation pattern was very noisy with two grid length scale waves. The most likely explanation for this feature is an interaction between the dynamics (numerics) and

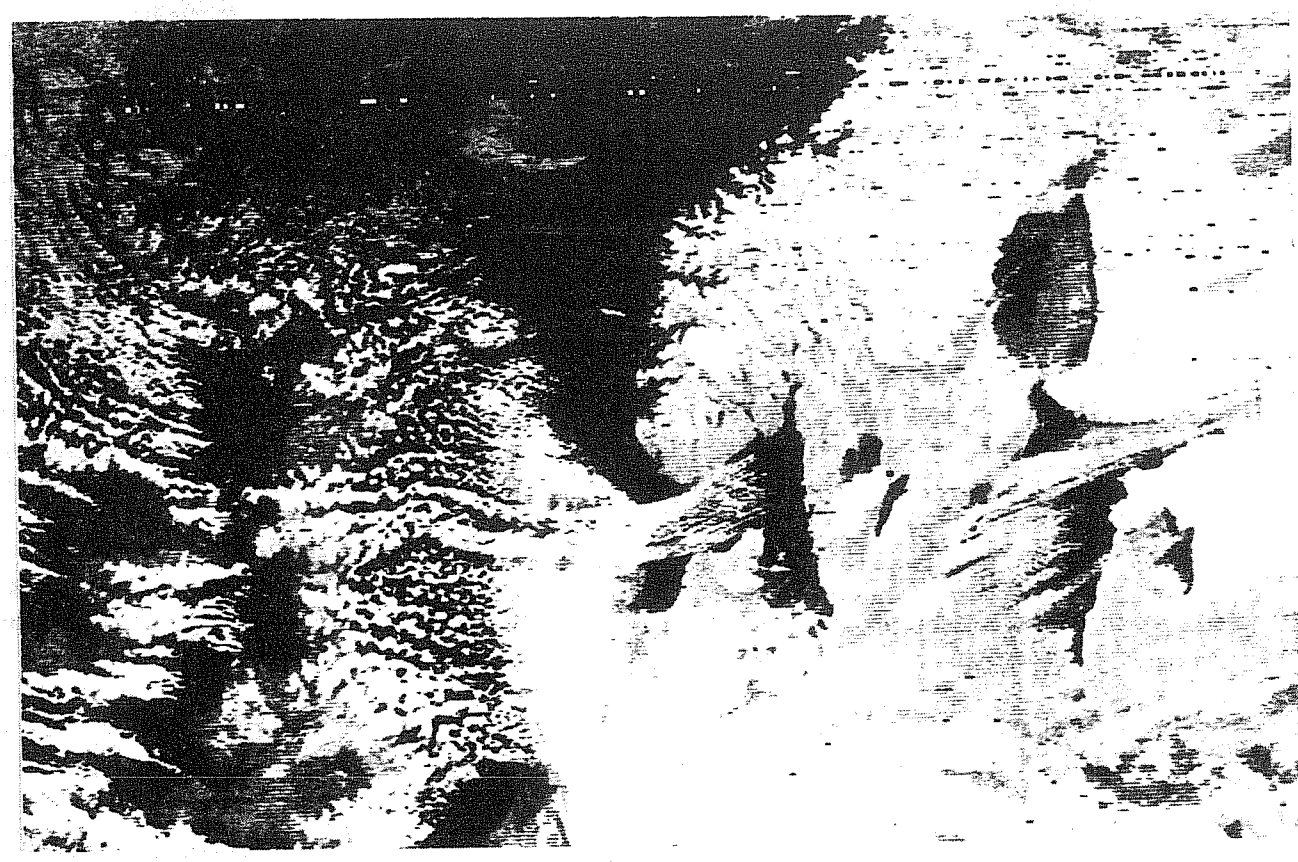

Figure 20: NOAA-10 IR 12 January 1987 18:11 UTC

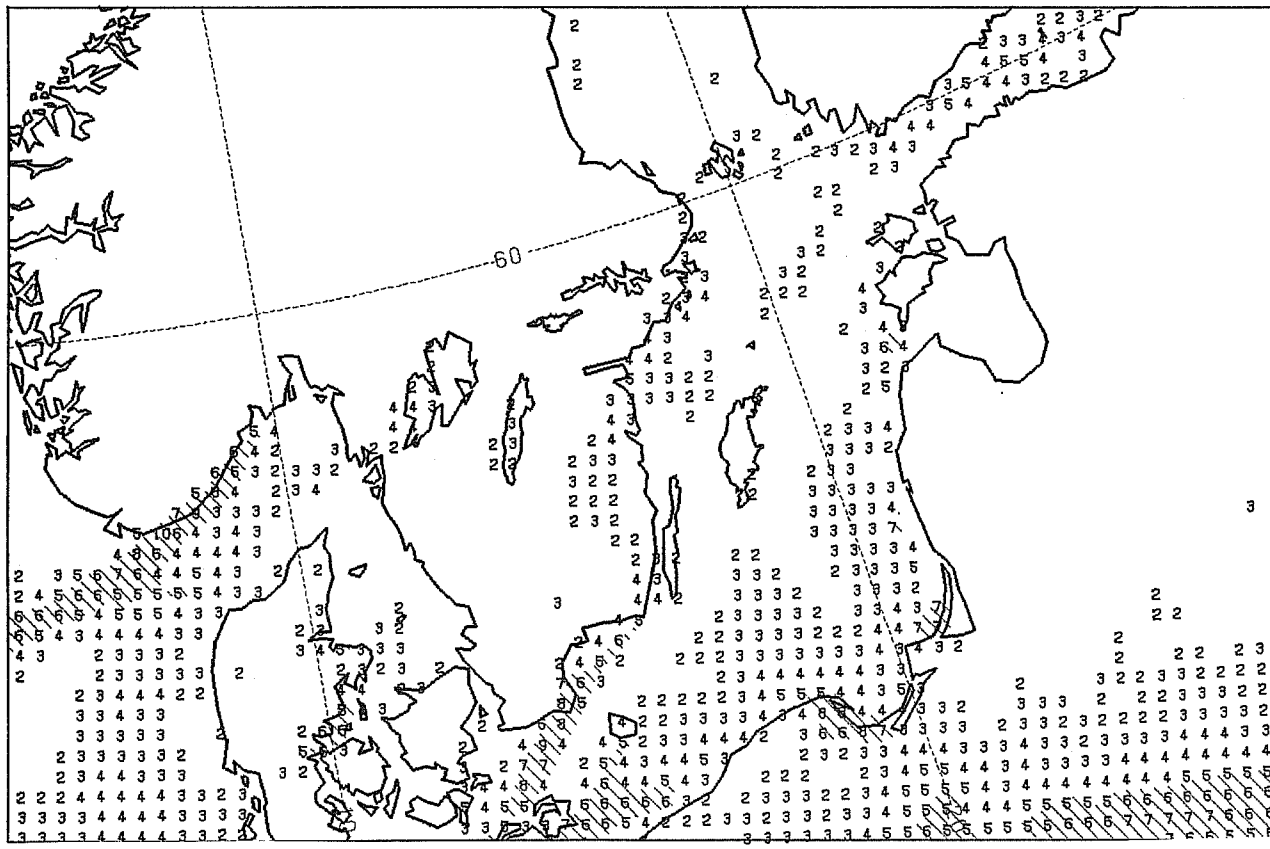

Figure 21: Experiment BT1, HIRLAM forecast of total precipitation, 12 January 1987 00UTC +06h - +18h; Climatological sea ice and SST initial data.

the Kuo convection scheme. The numerical scheme causes some low-amplitude two grid-length scale noise that will feed the Kuo convection scheme with moisture convergence on the same horizontal scale. The Kuo scheme will then act to amplify these short wave disturbances and once created they will remain and amplify. Since they are on the two grid-length scale, they will remain stationary. The results of the forecast experiment demonstrates that the second order horizontal diffusion scheme is not able to remove this short wave noise efficiently, which can also be understood from the corresponding filtering response function. An experiment with the linear fourth order horizontal scheme resulted in more organized precipitation patterns and was without the two grid length scale noise noticed for the experiment with the second order scheme. This supports the hypothesis of an interaction between the dynamic/numerics and the Kuo scheme as the origin of the noise problems. The fourth order horizontal diffusion scheme was used for the remaining experiments of the study.
- The meteorological situation in the case studied was relatively stationary and it may therefore be assumed that the most important process is the flux of heat and moisture from the warm water surfaces of the Baltic Sea. This also means that details of the initial atmospheric analysis fields are likely to be less important. Experiments with and without data assimilation confirmed this hypothesis.

As indicated above, the horizontal resolution of forecast experiments discussed above (0.5 degree) does not permit a detailed description of the forcing from the warm water surfaces of the Baltic Sea, with its many bays and islands. Therefore a forecast experiment BT1 with a horizontal resolution of 0.2 degree was carried out. The orography, the land-sea mask, the climatological sea surface temperature and sea ice fields as well as other physiographical fields were derived directly for the higher resolution run from the US Navy and ECMWF climatological data bases. Initial atmospheric data were derived by a horizontal interpolation from the HIRLAM 0.5 degree analysis fields followed by a vertical interpolation to the model levels as determined from the higher resolution orography field. Normal mode initialization on the high resolution data was carried out as well. The high resolution forecast was obtained without any particular problems, although with a somewhat increased gravity wave noise level during the initial few hours of the forecast model integration.

As expected, the precipitation from the high resolution BT1 forecast (Figure 21) is more detailed than for the lower resolution forecast runs. A band of precipitation is formed along the trajectory of cold air over the Gulf of Finland and the central Baltic Sea. Also over the Bay of Riga, over the North Sea and over the Sea of Kattegatt, convective precipitation is forecasted in agreement with observations. Details of the precipitation patterns near the Swedish east coast and over the inland lakes of Vänern and Vättern are not so well forecasted, however.

Since the sea-surface temperature and sea-ice conditions of the Baltic Sea were quite different from the rather crude climatology fields used for the experiments described above, an attempt was made to utilize observed SST and sea ice data in a forecast experiment BT2. For this purpose, the meso-scale SMHI analyses of SST and sea ice were utilized. The main input data source for these meso-scale analyses are digitalized spot values taken from manual analysis maps produced twice a week at SMHI. The main differences between the climatological and observed data were: (1) The Gulf of Finland was more completely covered with ice in the observed state than in the climatological state, (2) There were some ice covered areas in the archipelago along the Swedish east coast and in lake Vänern in the observed state but not in the climatological state.

The introduction of initial observed SST and sea ice data in experiment BT2 resulted in a significant positive impact on the precipitation forecast, as can be seen in figure 22. The structure of the main convective precipitation band over the central Baltic Sea is very well forecasted. Notice particularly the delay, compared to experiment BT1, in convective activities along trajectories over the Gulf of Finland due to introduction of increased ice cover and the "hole" in the convection along the Swedish east coast

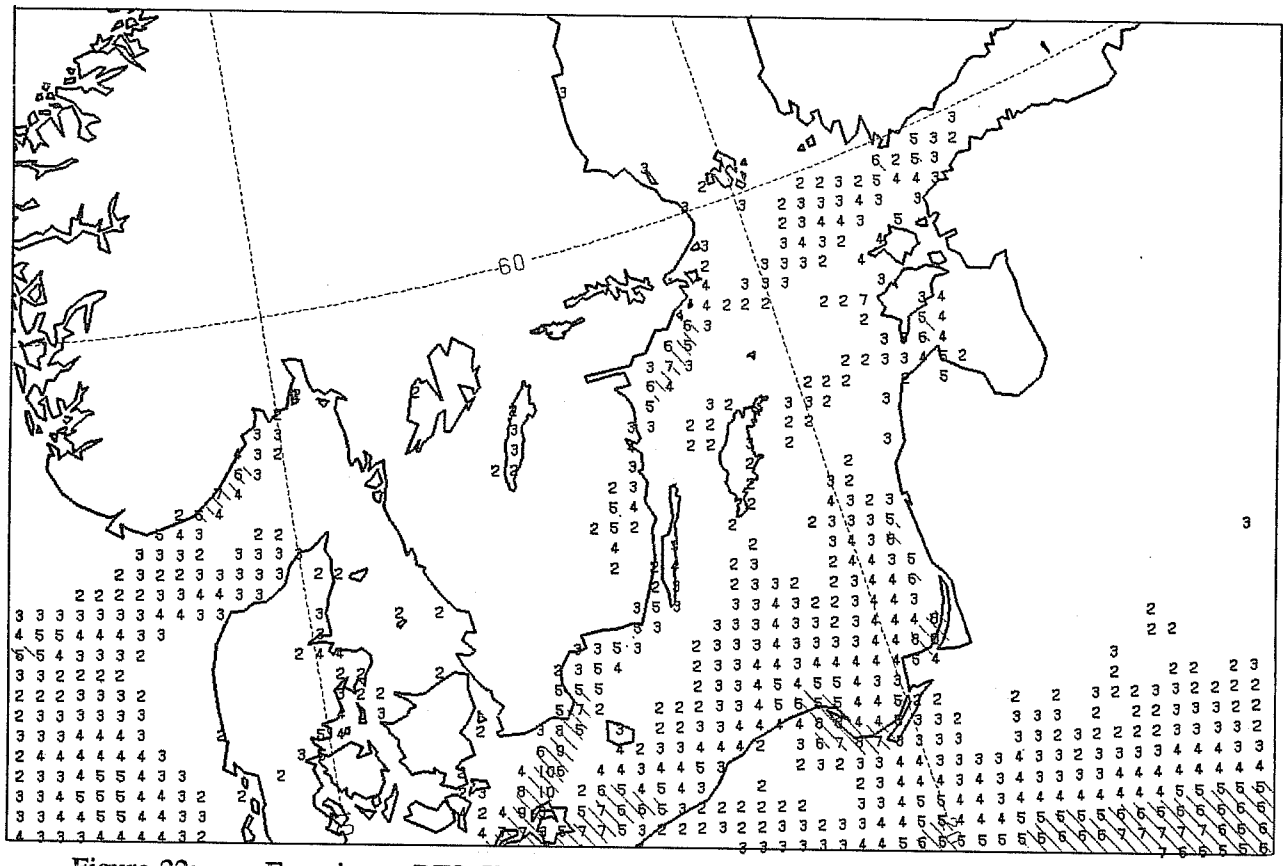

Figure 22: Experiment BT2, HIRLAM forecast of total precipitation, 12 January 1987 00UTC +06h - +18h; Analysed sea ice and SST initial data.

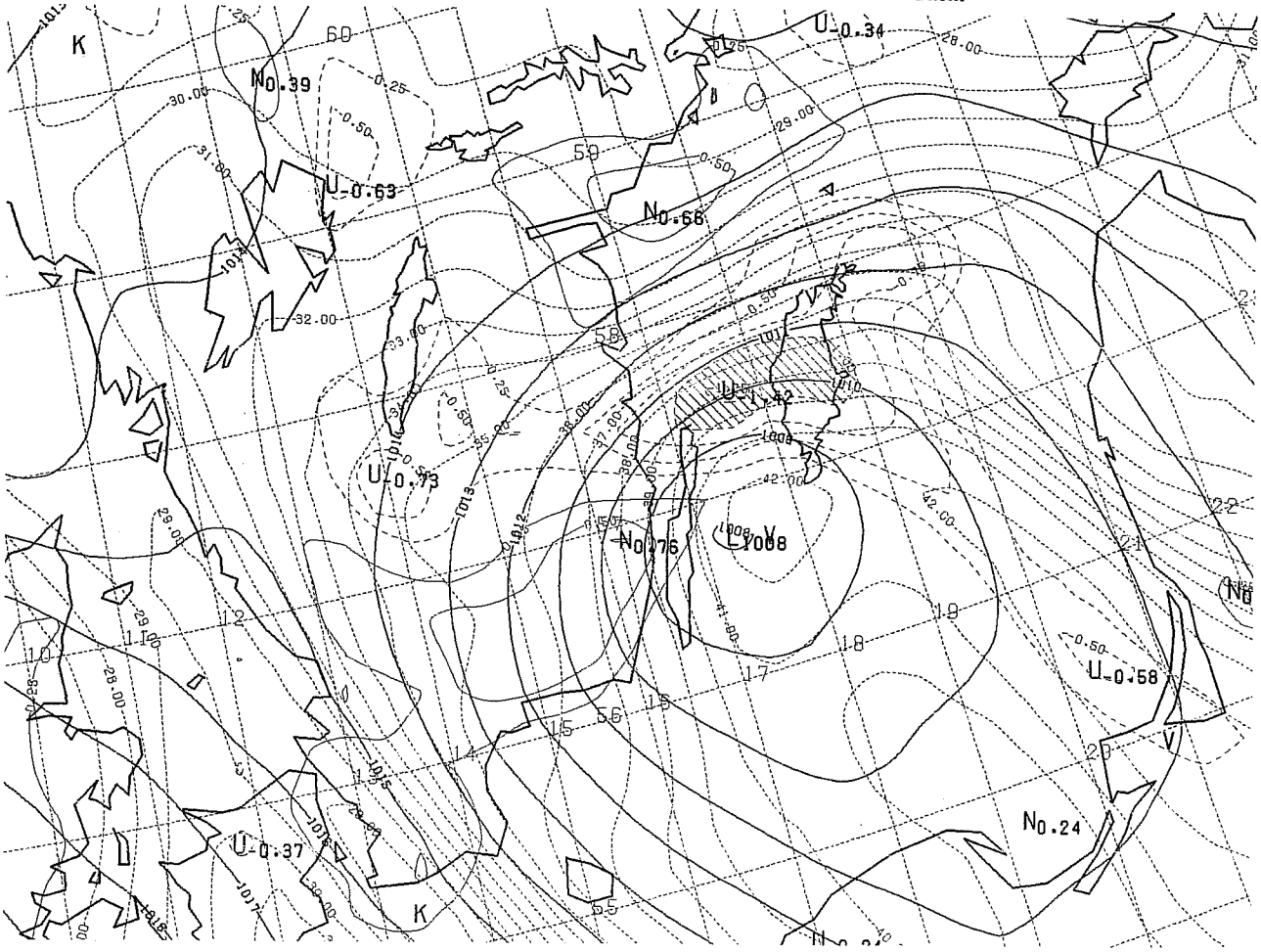

Figure 23: High resolution HIRLAM gridpoint model forecast. 23 July 1985 + 18h. Mean sea-level pressure, eq.pot.temperature and omega at 850 hPa.

just north of the main convection band.

In summary, the HIRLAM forecasting system was applied on a very high horizontal resolution for a case study with flow of very cold air over the relatively warm water surfaces of the Baltic Sea. Although the vertical resolution of the forecast experiments was far from being consistent with this high horizontal resolution and although no special attention was spent on tuning of the physical parameterization schemes, the forecast model proved to be able to simulate quite well the formation of bands of convective activities over the Baltic Sea. This must be considered to be very promising for the future with regard to research (and operational) application of the HIRLAM system at meso-scale resolutions.

4.1.2 The Baltic Bomb - 23 July 1985

As a testcase a notorious storm over the southern Baltic Sea on July 23rd 1985 was chosen. The prime purpose of this experiment was to explore the possible problems connected with resolutions of the order 25 km, but we were also interested in trying to get an insight into the cause of the event. The Baltic Storm developed rapidly in the morning of July 23rd from an existing weak low over the Danish island of Funen. In the afternoon it had developed into an intensive mesoscale cyclone near the northern tip of the Baltic island of Öland, with windspeeds exceeding 25 m/sec and precipitation exceeding 40 mm at several sites. The entire system had a diameter less than about 500km. The event was not predicted by available numerical forecasts at the time, and no gale- or storm warning was issued.

The runs were made on Cray-ECMWF, using ECMWF observations and analyses as lateral boundary conditions. First a data assimilation was run from July 21st 12UTC with a resolution of 0.5*0.5 deg. A +24h forecast from July 23rd 00UTC gave some indications of a development, but far from that observed. The 0.5*0.5 deg. analyses were interpolated to 0.2*0.2 deg. and a corresponding high resolution orography was extracted from the "Navy tape data". The vertical resolution was kept unchanged. In the "control" experiment, identical to the 0.5 degree run in everything but the resolution, an intensive cyclone developed. At +18h windspeeds of 18 m/sec were found at the second lowest model level about 150 m above ground, and over 12 hours more than 30 mm of precipitation was released. Figure 23 shows the +18h forecast of surface pressure, surface winds and vertical velocity at 850 hPa.

The synoptic background for the intense development was a narrow tongue of very warm and moist tropical air penetrating into the initial low from the south. A very short wave trough in the upper troposphere was approaching from the northwest. This feature could be identified in potential vorticity analyses over northern Iceland already 36 hours before the start of the event. When the potential vorticity maximum caught up with the low level tropical air a rapid development began. In the mature state 18 hours later, the cyclone was characterized by intense ascending motion with stratiform precipitation and release of latent heat. A characteristic feature was the shallowness of the storm, very little was to be seen above 700 hPa. Superficially the Öland storm reminds of a Polar Low, but since there are no appreciable sea-air temperature contrasts, the energy can not come from surface fluxes but rather from the initial moist potential energy. Hence the storm dies very rapidly after the energy has been released, after another 12 hours not much is to be seen in the analyses. The primary effect of the high resolution is to concentrate the area of low level convergence and ascending motion, thereby allowing a much more intense latent heat release than in the 0.5 deg forecast. Improved coastal convergence due to the high resolution land-sea mask is also likely to contribute.

There are clear indications that slantwise convection is a crucial process. In a set of sensitivity experiments the relative importance of the stratiform and the convective (Kuo-type) precipitation release was investigated. This was done either by switching one or the other completely off, or with a tuning parameter for the efficiency of stratiform release. When the stratiform process dominates, the model

atmosphere is unstable to slantwise (but not to vertical) moist convection and yields the most intense development. In runs where the Kuo scheme is dominating the resulting vertical mixing removes the slantwise instability and reduces the overall development. It is concluded from these experiments that further work is needed on the treatment of slantwise convection. We find it encouraging that high resolution forecasts from lower resolution analyses are able to add details only due to better representation of sharp gradients and surface orography.

4.2 A spectral HIRLAM formulation

Considering the successful application of the spectral transform technique for global forecast models, there has been an aim within the HIRLAM project to develop a spectral version of the HIRLAM multi-level model. The initial steps were taken by Machenhauer and Haugen (1987), who developed a spectral limited area shallow water model based on the idea of extending the limited area in the two horizontal dimensions in order to obtain periodicity in these two dimensions and to permit the use of efficient Fast Fourier Transforms. The same idea has now been implemented into the full multi-level HIRLAM framework.

Alternative techniques for spectral limited area models have been applied at ECMWF (Simmons 1984, Hoyer 1987) and at the Japanese Meteorological Agency (Tatsumi 1986). The ECMWF approach is based on treating the deviations from the large scale forecast only as the forecast model variables. Since these deviation variables vanish at the lateral boundaries, trigonometric transforms can be utilized. The drawback of the ECMWF approach is the need to handle large-scale background fields for each timestep over the whole limited area and the need to add extra forecast model terms for interaction between the background fields and the model (deviation) fields. The JMA approach is based on a special treatment of the variation of the fields between the boundary values by introduction of an extra wave component. The drawback of this approach is that the basis functions do not form an orthogonal set.

The same basic continuous model equations, the same vertical differencing scheme, the same upper and lower boundary conditions and the same physical parameterization schemes as described above for the HIRLAM Level 1 model are utilized for the spectral HIRLAM model.

4.2.1 The area extension technique

The geometry of using an extension zone to obtain periodic variations in both horizontal dimensions of the forecast model variables is illustrated in Figure 24. Assume that we want to represent a boundary field f, given in the gridpoints of the inner "integration area" only, by a bi-periodic Fourier-series. To do so, extrapolated grid-point values are determined in the extension zone in such a way that the subsequent Fourier transform will give a smooth representation in the inner integration area with preserved normal gradients along the lateral boundaries. This is achieved by an extrapolation procedure, first along each row of gridpoint values in the x-direction and then along each column of gridpoint values in the extended area in the y-direction. The extrapolation is carried out with the constraint that the normal gradients and the absolute values are preserved at the boundaries of the inner integration area. With these constraints, it is needed to determine 4 coefficients in a functional representation of the extrapolation. To achieve best possible consistency with the spectral Fourier series representation, sin- and cosine- functions are utilized for this extrapolation.

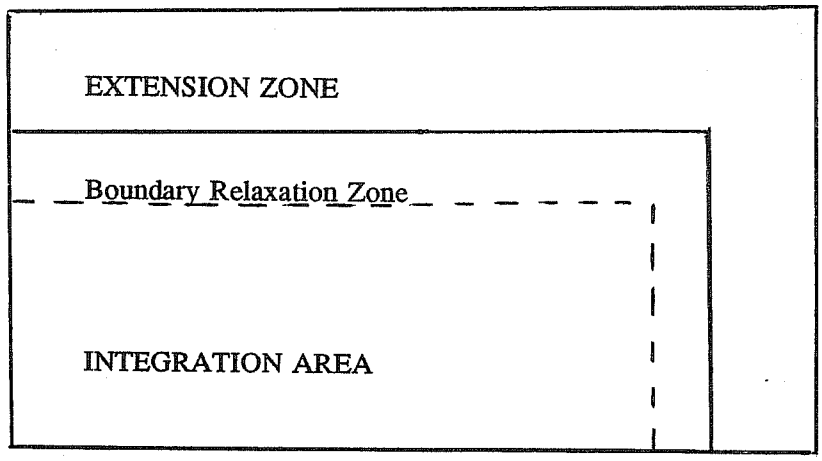

Figure 24: Inner integration area, boundary relaxation zone and extension zone as used by the spectral HIRLAM model

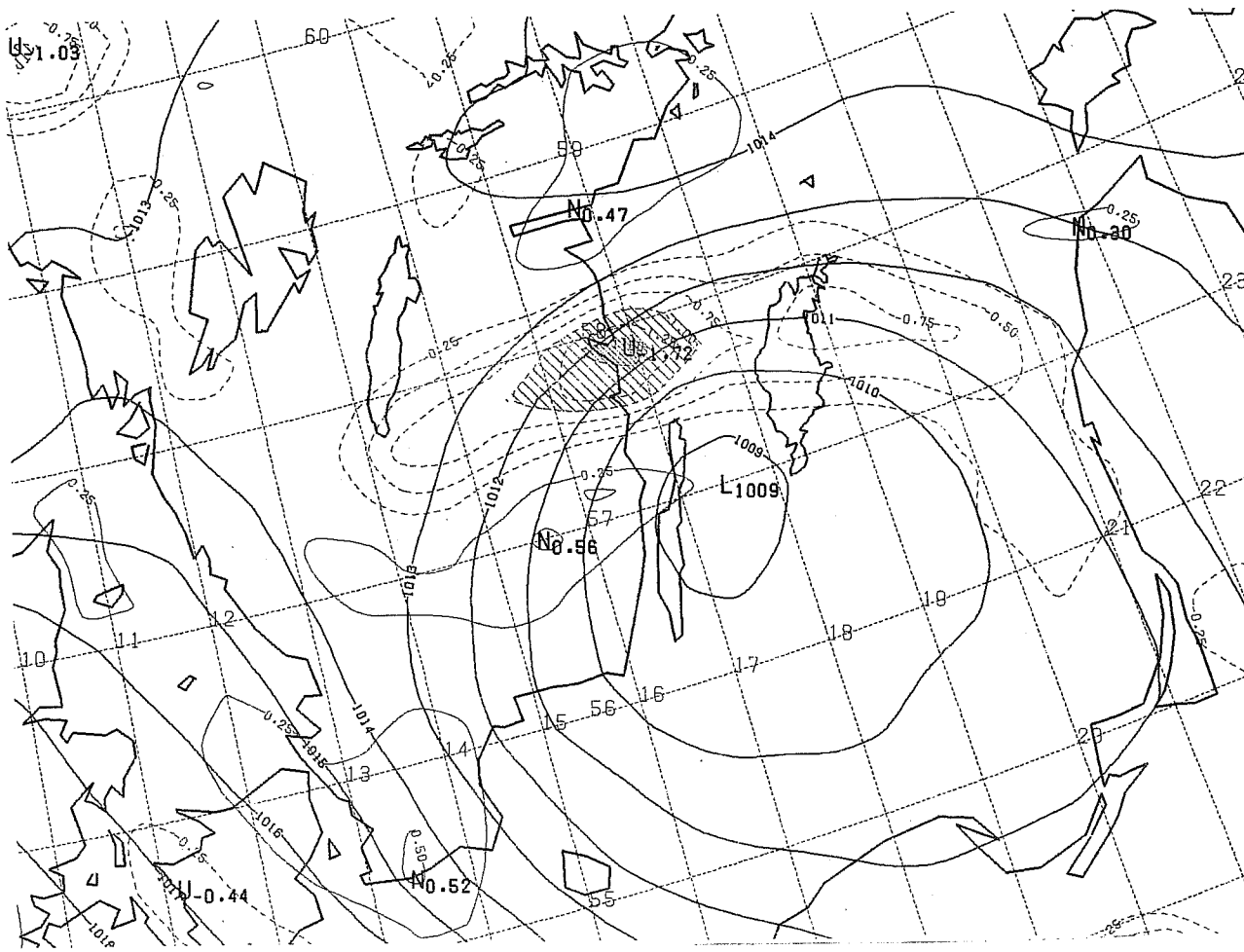

Figure 25: High resolution HIRLAM spectral model forecast. 23 July 1985 + 18h. Mean sea-level pressure and omega at 850 hPa.

4.2.2 Spectral truncation considerations

To obtain an aliasing-free computation of quadratic terms in the transform grid, this grid should include at least 3*M+1 grid-points in one direction if M is the number of complex Fourier-components of the spectral model in that particular direction. However, in the present formulation of HIRLAM-model, these quadratic terms also include map-factors as in e.g. $U\frac{1}{h_x}\frac{\partial U}{\partial x}$. This needs to be considered in the determination of the transform grid. Thus if the inverse map factors are truncated by N waves, the transform grid (covering the extended area) should contain at least 3*M+N+1 gridpoints. Also, the truncation of the boundary relaxation factor needs to be considered in the design of the transform grid.

In addition, an "elliptic" spectral truncation defined by $(M_y/M_x)^2 m_x^2+m_y^2 \le M_y^2$ that gives an isotropic and homogeneous resolution over the extended area is being utilized for the present experiments.

4.2.3 Normal modes, non-linear normal mode initialization and the normal mode time-stepping

The vertical normal modes of the spectral HIRLAM model were derived for two purposes - to be used for non-linear normal mode initialization and to be used in the time integration scheme based on initialization of the gravest vertical modes each time step. For the derivation of the normal modes, the model is linearized around a basic state at rest, with a constant surface pressure and with a constant temperature at each model level. In addition, the Coriolis parameter and the map-factors are assumed to have there areal mean values in the derivation of the normal modes. The assumption of constant map factors is a simplification as compared to the initialization of the HIRLAM Level 1 gridpoint model. It was introduced in order to be able to utilize the spectral basis functions also for the horizontal representation of the normal modes to avoid further horizontal transformations from the spectral to the normal mode space. Tests of the initialization and the normal mode time stepping scheme do not indicate that this further simplification introduces any particular problems.

The basis for the non-linear normal mode initialization is the Machenhauer balance condition that the tendencies of the gravest gravity modes are zero. The iteration technique suggested by Machenhauer to obtain this balance is utilized. Utilizing the simplifications in the derivation of the normal modes as mentioned above this iteration takes a quite simple form:

$$\Delta u_{lmn}=\frac{1}{\sigma^2_{lmn}}\{\bar{f}\dot{v}_{lmn}-i\frac{m'}{\bar{h}_x}\dot{P}_{lmn}\}$$

$$\Delta v_{lmn}=\frac{1}{\sigma^2_{lmn}}\{-\bar{f}\dot{u}_{lmn}-i\frac{n'}{\bar{h}_y}\dot{P}_{lmn}\}$$

$$\Delta P_{lmn}=-\frac{i\bar{\Phi}_l}{\sigma^2_{lmn}}\{\frac{m'}{\bar{h}_x}\dot{u}+\frac{n'}{\bar{h}_y}\dot{v}\}$$

where l denotes vertical mode number, m and n horizontal wave numbers , σ_{lmn} frequency of the mode, $\dot{x}$ model tendency of a variable computed by the full non-linear model at a certain iteration and Δx the corresponding correction in the initialization iteration scheme. P is a linear combination of ln(ps) and the model level temperatures. Normally it is sufficient with 2 iterations in the initialization of the gravest few modes to get a satisfactory initial balance.

As an alternative to the semi-implicit scheme, Daley (1980) proposed and tested a time stepping scheme based on normal mode initialization to make it possible to run the primitive equation models with longer time-steps than dictated by the frequency of the fastest gravity modes as in an explicit time stepping scheme. The rationale behind the normal mode scheme is the same as behind the non-linear normal mode initialization scheme, i.e. that the tendencies of the fastest gravity modes are small. Thus the basic idea is to initialize the gravest gravity modes each time step with an initialization scheme as described above.

In any practical implementation of the normal mode time stepping scheme it is not possible to carry out several iterations to obtain the balance of the gravity modes each time step since the needed tendency calculations would be too expensive. Based on the assumption that the tendencies of the fastest gravity modes are small, a reasonable simplification is to replace the (unbalanced) gravity modes forecasted by e.g. a leap-frog scheme to timestep $t+\Delta t$ by the corresponding gravity modes at timestep t as balanced by 1 iteration only. By this approach, no extra tendency calculations are needed. This type of time stepping scheme was introduced into the spectral HIRLAM model. In symbolic form, this time stepping of the fast modes combined with a leap-frog scheme for the slower modes, could be described as follows:

$$\tilde{\varphi}^{t+\Delta t} = \varphi^{t-\Delta t} + 2\Delta t \phi^{t}$$

$$\varphi^{t+\Delta t} = \tilde{\varphi}^{t+\Delta t} - \tilde{\varphi}^{t+\Delta t}_{fast} + \varphi^{t}_{bal.fast}$$

In order to minimize the number of vertical transforms, the time integration scheme has been programmed in the following form:

$$\varphi^{t+\Delta t} = \varphi^{t-\Delta t} + 2\Delta t \{\phi^{t} - \phi^{t}_{fast} + \frac{\varphi^{t}_{fast} - \varphi^{t-\Delta t}_{fast}}{2\Delta t} + \frac{\Delta\varphi_{init,fast}}{2\Delta t}\}$$

4.2.4 Flow of computations

In the present formulation, the following steps of computation are carried out during each time-step of the model integration. At the start of the time step the "dynamical" variables $\hat{u}, \hat{v}, \hat{T}, \hat{q}, \ln\hat{p}_s$ in spectral space and the physical variables $T_s, T_{sd}, W_s, W_{sd}, S_n$ in grid-point space are assumed to be available at timesteps t and $t-\Delta t$.

Step 1:
Carry out Fourier-transforms to obtain grid-point values in the transform grid of the following variables

$$u, \frac{\partial u}{\partial x}, \frac{\partial u}{\partial y}, v, \frac{\partial v}{\partial x}, \frac{\partial v}{\partial y}, T, \frac{\partial T}{\partial x}, \frac{\partial T}{\partial y}, q, \frac{\partial q}{\partial x}, \frac{\partial q}{\partial y},$$

$$\ln(p_s), \frac{\partial \ln(p_s)}{\partial x}, \frac{\partial \ln(p_s)}{\partial y} \quad \text{at time t.}$$

Step 2:
Compute (explicit) dynamical tendencies

$$\frac{\partial u}{\partial t}, \frac{\partial v}{\partial t}, \frac{\partial T}{\partial t}, \frac{\partial q}{\partial t}, \frac{\partial \ln(p_s)}{\partial t}$$

at time t.

Step 3:

Carry out Fourier-transforms to obtain grid-point values in the transform grid of $u, v, T, q, \ln(p_s)$

at time $t-\Delta t$.

Step 4:
Compute physical tendencies

$$\frac{\partial u}{\partial t}, \frac{\partial v}{\partial t}, \frac{\partial T}{\partial t}, \frac{\partial q}{\partial t}, \frac{\partial T_s}{\partial t}, \frac{\partial T_{sd}}{\partial t}, \frac{\partial W_s}{\partial t}, \frac{\partial W_{sd}}{\partial t}, \frac{\partial S_n}{\partial t}$$

at time $t-\Delta t$. Some of the parameterization schemes also use dynamical tendencies to derive values

valid at time $t+\Delta t$.

Step 5:
Extend the tendency fields from the inner integration area by boundary relaxation towards the area extended geostrophical tendencies of the lateral boundary fields.

Step 6:
Fourier transform of the sum of dynamical and physical tendency fields to spectral space:

$$\frac{\partial \hat{u}}{\partial t}, \frac{\partial \hat{v}}{\partial t}, \frac{\partial \hat{T}}{\partial t}, \frac{\partial \hat{q}}{\partial t}, \frac{\partial \ln(\hat{p}_s)}{\partial t} .$$

Step 7:

Compute horizontal diffusion tendencies $\frac{\partial \hat{u}}{\partial t}, \frac{\partial \hat{v}}{\partial t}, \frac{\partial \hat{T}}{\partial t}, \frac{\partial \hat{q}}{\partial t}$ at time $t-\Delta t$.

Step 8:
Timestepping and timefiltering to obtain new (preliminary) values

$\hat{u}, \hat{v}, \hat{T}, \hat{q}, \ln(\hat{p}_s)$, T_s, T_{sd}, W_s, W_{sd}, S_n

at time t and $t+\Delta t$.

Step 9:
Carry out boundary relaxation by Fourier transforms to grid-point space, relaxation towards the area extended lateral boundary fields and Fourier transforms back to spectral space of new values of the following fields: $\hat{u}, \hat{v}, \hat{T}, \hat{q}, \ln(\hat{p}_s)$

4.2.5 Accuracy and efficiency tests

A series of tests to compare the spectral HIRLAM model with the grid-point model with regard to accuracy and computing economy have started . Preliminary tests on a strong synoptic scale storm development (3 February 1991 near Iceland) seem to indicate that if the shortest wave in the spectral model is selected to correspond to 4 grid-lengths of the gridpoint model, the accuracy of the resulting forecasts are very similar. The computing time for a particular 24 h run with 110*100*16 gridpoints and a 6 min. timestep in the gridpoint-model was 424 seconds (1 Cray YMP processor) and the corresponding computing time for the spectral model with 82*74*16 gridpoints in the (inner) transform grid and a time-step of 6 min. 40 sec. was 332 seconds. Thus, the spectral HIRLAM model seems to be competitive with the grid-point HIRLAM model with regard to computing economy. A test-run on the mesoscale Öland-storm (Figure 25) discussed above seems to indicate, however, that somewhat higher spectral resolution than 1 wave per 4 gridlengths is needed to compete with the grid-point model. However, considerations about needed horizontal diffusion etc. for the two models have to be taken into account. It should also be mentioned that there exist potential for further significant reductions of computing time in the spectral model. There is e.g. a possibility to carry out the boundary relaxation in spectral space by storing the boundary tendency fields multiplied by the boundary relaxation factors in spectral space. If this is possible, the FFTs in "Step 9" are not needed.

4.3 The development of the HIRLAM Level 2 system

The HIRLAM Level 2 project will be ended in December 1990. The main goal during this remaining time of the HIRLAM 2 Project is to develop a HIRLAM Level 2 system superior to the present HIRLAM Level 1 system. The main new components of the Level 2 system are (or will be):

(1) A re-coded version of the physical parameterization package that fulfills the recommendations suggested by Kalnay et.al.(1989) has been programmed and tested. Thus, all input fields are provided as formal parameters in the call to the physics subroutines and COMMON is used for physical constants only.

(2) A new dynamical/numerical part of the model code, which allows for Eulerian or Semi-Lagrangian advection as well as three- or two-time level time schemes has been developed. Variable temporal time-stepping for physics will be included.

(3) A unified program package for the pre-processing of lateral boundary values and the post-processing will be introduced into the forecast model code.

(4) The Sundqvist condensation scheme is being introduced into the recoded model.

(5) Improved observational quality control algorithms by the use of individual observational error statistics.

(6) Analysis of surface parameters including snow, sea ice, SST, 2 meter temperature, humidity and soil moisture.

(7) An improved surface parameterization scheme (treatment of vegetation)

The importance of the first action, although very dull and tedious, could not be over-estimated. The HIRLAM Level 1 physics package was programmed in the old ECMWF CDC 6600 style with the use of lots of COMMON areas and a huge BUF-area for all the model variable fields. It was very difficult for a non-specialist to touch this code and the exchange of subroutines for one particular physical process with another model group was not to consider. The re-programming effort took about one man-year, but it was certainly worth the effort. The Meteo France modelling group has carried out a similar re-programming of the ARPEGE physical parameterization package and this package was made available to the HIRLAM project for comparison purposes. It turned out that the interfaces to the two physical parameterization packages were very similar. Thus, after only 2 weeks of programming and testing is was possible to run the HIRLAM model with the ARPEGE physics. Some interesting characteristics of the behavior of the ARPEGE physics within the HIRLAM framework have already been noticed and it is the intention to carry out physics "transplantation" experiments where the subroutine for one particular physical process is replaced by the ARPEGE version while keeping the other processes in their HIRLAM formulation. In this way, it is hoped to cast some light on e.g. the low level temperature bias problem as experienced in the operational application of the HIRLAM system.

5. Summary and future work

The coordinated efforts among the small weather services within the HIRLAM community have made it possible to develop and maintain a modern system for high resolution limited area data assimilation and forecasting. The weather services of Finland and Denmark are already using this system for production of operational numerical forecasts which are used and highly appreciated by the weather forecasting teams. The quality of these operational numerical forecasts have proven to be at least as good as those from major European forecasting centers.

These coordinated efforts in numerical weather prediction will continue within the framework of the HIRLAM 3 project to be established in 1992. A cooperation between the HIRLAM 3 project and the modelling group of Meteo France is planned for particular research problems and tasks, e.g. development of a meso-gamma scale non-hydrostatic model and parameterization of physical processes in general.

Acknowledgements

Results presented here have been obtained within the framework of the HIRLAM project and I am grateful to all my HIRLAM colleagues for their contributions. In particular I am grateful to my colleagues at FMI and DMI for their results from the operational applications of the HIRLAM system. I would also like to thank Bennert Machenhauer for his stimulating support during the development of the spectral HIRLAM model and Per Kållberg for results from the "Baltic Bomb" experiment and for constructive comments on this manuscript.

References

Andersen, J.H., 1977:
A routine for normal mode initialization with nonlinear correction for a multi-level spectral model with triangular truncation. ECMWF Internal Report No. 15, 41pp.

Andersson, T. and S. Nilsson, 1990:
Topographically Induced Snowbands over the Baltic Sea and Their Precipitation Distribution. Weather and Forecasting, Vol.5, NO.2, June 1990.

Arakawa, A., 1966:
Computational design for long-term numerical integration of the equations of fluid motion: two-dimensional incompressible flow. Part 1. J. Comp. Phys., 1, 119-143.

Bijlsma, S.J. and L.M. Hafkenscheid, 1984:
A non-linear normal mode initialization method for a limited area. Internal KNMI Note, De Bilt, The Netherlands, 38pp.

Daley, R., 1980:
The development of efficient time integration schemes, using model normal modes. Mon. Wea. Rev., 108, 100-110.

Gandin, L.S., 1963:
Objective analysis of meteorological fields. Moscow 1963 (in russian). Translation from russian by the Israeli Program for Scientific Translations (1965).

Hoyer, J.-M., 1987:
The ECMWF spectral limited area model. In Workshop Proceedings: Techniques for horizontal discretization in numerical weather prediction models; ECMWF, 2-4 November 1987, 343-360.

Kalnay, E. et.al., 1989:
Rules for interchange of physical parameterizations. Bull. of the A.M.S., Vol.70, No.6, 620-622.

Kuo, H.L., 1974:
Further studies of the influence of cumulus convection on large-scale flow.
J. Atmos. Sci., 31, 1232-1240.

Kållberg, P. and R. Gibson, 1977:
Lateral boundary conditions for a limited area version of the ECMWF model. WGNE Progress Report No. 14. WMO Geneva.

Kållberg, P. (editor), 1989:
The HIRLAM Level 1 Forecast Model Documentation Manual. Available from SMHI, S-60176 Norrköping, Sweden.

London,J., and T. Sasamori, 1968:
A brief note concerning radiative cooling as a function of temperature and water vapor. WMO Technical Report No. 104, pp. 488-489.

Lorenc, A., 1981:
A global three-dimensional multivariate statistical interpolation scheme. Mon. Wea. Rev. 109, 701-721.

Louis, J.F., M. Tiedtke and J.-F. Geleyn, 1981:
A short history of operational PBL-parameterization at ECMWF. ECMWF Workshop on Planetary Boundary layer Parameterization, Nov. 1981, 59-79.

Machenhauer, B., 1977:
On dynamics of gravity oscillations in a shallow water model with applications to normal mode initialization. Contrib. Atmos. Phys. 50, 253-271.

Machenhauer, B. and J.E. Haugen, 1987:
Test of a spectral limited area shallow water model with time-dependent lateral boundary conditions and combined normal mode/semi-Lagrangian time integration schemes. In Workshop Proceedings: Techniques for horizontal discretization in numerical weather prediction models; ECMWF, 2-4 November 1987, 361-377.

Majewski, D., 1985:
Balanced Initial and Boundary Values for a Limited Area Model. Beitr.Phys.Atm.,Vol.58,No.2.,May 1985.

Sadourny, R., 1975:
The dynamics of finite difference models of the shallow-water equations. J. Atmos. Sci., 32, 680-689.

Simmons, A.J., and D.M. Burridge, 1981:
An energy and angular momentum conserving vertical finite-difference scheme and hybrid vertical coordinates. Mon. Wea. Rev., 109, 758-766.

Simmons, A., 1984:
A Spectral Limited Area Model. ECMWF Internal Memorandum, 35 pp.

Tatsumi, Y., 1986:
A spectral limited-area model with time-dependent lateral boundary conditions and its application to a multi-level primitive equation model. J. of Met. Soc. Japan, 64, 637-664.